The Abdus Salam
International Centre for Theoretical Physics

United Nations Educational, Scientific and Cultural Organization

IAEA International Atomic Energy Agency

**ADVANCED WORKSHOP ON**
***"ANDERSON LOCALIZATION, NONLINEARITY AND TURBULENCE: A CROSS-FERTILIZATION"***

**23 August - 3 September 2010,**
**ICTP, Trieste, Italy**

**Organizers:**

**B. ALTSHULER, G. FALKOVICH, S. FLACH, K.R. SREENIVASAN and V.E. KRAVTSOV**

# LIST OF
# POSTER PRESENTATION ABSTRACTS

The Abdus Salam
International Centre for Theoretical Physics

**ADVANCED WORKSHOP ON**
***"ANDERSON LOCALIZATION, NONLINEARITY AND TURBULENCE: A CROSS-FERTILIZATION"***
**23 August - 3 September 2010, ICTP, Trieste, Italy**

# LIST OF POSTER PRESENTERS

**Mohsen AMINI ABCHUYEH**
Anderson transition in disordered graphene

**Irina BASHKIRTSEV**
Stochastic sensitivity and transition to chaos

**Alexander BERSHADSKII**
Chaos from turbulence: stochastic-chaotic equilibrium in turbulent convection

**Joshua BODYFELT**
One parameter scaling theory for stationary states of disordered nonlinear systems

**Hosein CHERAGHCHI**
Localization-delocalization transition through graphene superlattice with long-range correlated disorder on potential barriers

**Dmitry CHURKIN**
Turbulent square-root broadening of fiber lasers output spectrum

**Leonardo ERMANN**
Turbulent ratchet transport of interacting particles

**Roman KATZER**
Real-space renormalization group for Anderson localization of interacting electrons in the Anderson-Hubbard model

**Ramaz KHOMERIKI**
Interaction induced fractional Bloch and tunneling oscillations

**Dmitry KRIMER**
Impact of nonlinearity on Anderson and Wannier-Stark localization

**Yoav LAHINI**
Anderson localization and nonlinearity in disordered and incommensurate photonic lattices

**Tetyana LAPTYEVA**
Evolution of wave packets in nonlinear disordered media: strong chaos and asymptotic weak spreading regimes

**Gabriel LEMARIE**
Experimental observation of the Anderson transition with matter waves

**Luca MORICONI**
Cascade picture and extended self-similarity in electron localization

**Mario MULANSKY (two posters)**
Localization in systems with disorder and strong nonlinearity
Thermalization in short random nonlinear lattices

**Felipe PINHEIRO**
Suppression of Anderson localization of light and Brewster anomalies in disordered superlattices containing a dispersive metalmaterial

**Ilia RUSHKIN**
Statistics of wavefunctions at Anderson transition in power-law random banded matrices

**Lev RYASHKO**
Stability and control for invariant manifolds of nonlinear stochastic systems

**Reza SEPEHRINIA**
Band center anomaly and single parameter scaling in one-dimensional Anderson localization

**Tomas TEITELBAUM**
Decay of turbulence in rotating flows

**Ilya VATNIK**
Cascade random distributed feedback fiber laster

A Letters Journal Exploring the Frontiers of Physics

August 2009

EPL, **87** (2009) 37002
doi: 10.1209/0295-5075/87/37002

www.epljournal.org

# Anderson transition in disordered graphene

M. Amini[1], S. A. Jafari[1,2(a)] and F. Shahbazi[1]

[1] *Department of Physics, Isfahan University of Technology - Isfahan 84154-83111, Iran*
[2] *The Abdus Salam ICTP - 34100 Trieste, Italy, EU*

received 31 May 2009; accepted in final form 21 July 2009
published online 25 August 2009

PACS 72.15.Rn – Localization effects (Anderson or weak localization)
PACS 72.20.Ee – Mobility edges; hopping transport
PACS 81.05.Uw – Carbon, diamond, graphite

**Abstract** – We use the regularized kernel polynomial method (RKPM) to numerically study the effect disorder on a single layer of graphene. This accurate numerical method enables us to study very large lattices with millions of sites, and hence is almost free of finite-size errors. Within this approach, both weak- and strong-disorder regimes are handled on the same footing. We study the tight-binding model with on-site disorder, on the honeycomb lattice. We find that in the weak-disorder regime, the Dirac fermions remain extended and their velocities decrease as the disorder strength is increased. However, if the disorder is strong enough, there will be a *mobility edge* separating *localized states around the Fermi point*, from the remaining extended states.



**Introduction.** – Graphene is the 2D allotrope of carbon in which carbon atoms with $sp^2$ hybridization are organized in a honeycomb lattice. Recently, the isolation of single graphene sheets has become possible through chemical exfoliation of bulk graphite [1–3], or epitaxial growth, either by chemical vapor deposition of hydrocarbons on metal substrates [4] or by thermal decomposition of SiC [5]. The latter method produces graphene layers with high crystalline quality. Properties such as, tuning the carrier types from hole to electron in the same sample through a gate voltage and remarkably high mobility of charge carriers, even at room temperature, due to the absence of back-scatterings, has made the graphene promising from the technological point of view in building the carbon-based electronic devices [6].

The electronic properties of pure graphene can be modeled with a simple tight-binding picture proposed by Wallace [7] which provides the essential band structure of graphene as a half-filled system with a density of states (DOS) vanishing linearly at the charge neutrality point. In this picture the energy dispersion is linear in momentum near the Fermi points, causing the quasi-particles behave as massless chiral Dirac electrons [8].

In spite of high crystalline quality, disorder cannot be avoided in currently available samples of graphene. Various kinds of intrinsic disorder such as surface ripples and topological defects, as well as extrinsic ones like vacancies, ad-atoms, charge impurities affect the electronic properties of graphene. The presence of a minimal conductivity at zero bias [2] implies the existence of extended states at the charge neutrality points, in contrast to prediction of the scaling theory in 2D [9].

There has been various theoretical and numerical approaches to study the effect of different types of disorder in graphene (as a review, see ref. [6] and references therein). Based on one-parameter scaling theory [10], Ostrovsky and coworkers found a metal-insulator transition in graphene for long-range disorder [11]. The hypothesis of one-parameter scaling was subsequently verified with numerical calculation of Bardarson *et al.* [12]. They used a transfer operator method to investigate the localization properties of the low-energy effective (Dirac) theory. Similar result for the beta function was obtained independently by Nomura *et al.* [13] by evaluating the Kubo formula for the conductance. Although these numerical works verify the hypothesis of single-scaling theory, but they predict that Dirac fermions remain delocalized at arbitrary strength of disorder. The effect of roughness on the electronic conductivity was studied in [14], and it was found that all states remain localized in the presence of random effective gauge fields induced by ripples.

Lherbier *et al.* used a real space and order $N$ Kubo formalism to calculate time-dependent diffusion constant $D(E,t)$ for the Anderson model on honeycomb lattice [15]. For small values of disorder strength $W$, they found

(a) E-mail: akbar.jafari@gmail.com

$D(E,t)$ saturates to a constant value in long-time limit, indicating the presence of extended states. At larger values of $W$ they report a decrease in $D(E,t)$ pinpointing the onset of localization.

Most of the analytical methods used in the studies of disorder in graphene, are able to handle restricted regimes of specific types of disorder. Their predictions are valid only on the low-energy scales around the Dirac points, where the inter-valley scatterings from the impurity potential can be ignored. When disorder strength becomes comparable to the band width, it is important to take into account all energy scales simultaneously along with possible interplay between different energy scales. There also remains an important question about whether there is a mobility edge in graphene in the strong-disorder regime or not.

In this paper we use the kernel polynomial method (KPM) [16] based on the expansion of spectral functions in terms of a complete set of polynomials to accurately calculate various spectral properties, including the density of states (DOS). The computation time in KPM method grows linearly with system size. Matrix manipulations can be done on the fly, which reduces the memory usage enormously. Therefore one can study very large lattice sizes in a moderate time. Regularization of KPM method known as RKPM remedies the Gibbs oscillations [17], and therefore is capable to handle *any type of disorder* with *arbitrary strength* in essentially the exact way. By this method, one can treat the low-energy and high-energy features of graphene on the same footing, and hence the interplay between the Dirac features and high-energy parts of the spectrum, as well as inter-valley scattering is taken into account. This method enables us to explore new regimes of disorder strength with fascinating properties.

**Model and method.** – From the single-particle point of view, disorder can affect the non-interacting electrons in graphene, mainly through spatial variations off on-site energy (diagonal disorder) or changes in the hopping integrals due to the variations in the distances or angles of the $p_z$ orbitals (off-diagonal disorder). In what follows we study the graphene with on-site uncorrelated disorder. We consider non-interacting electrons moving on a honeycomb lattice in the presence of local diagonal disorder. The basic model to describe this kind of problem is the Anderson model:

$$H = -t \sum_{\langle i,j \rangle} [c_i^\dagger c_j + \text{H.c.}] + \sum_j^N \epsilon_j c_j^\dagger c_j. \tag{1}$$

The first term describes hopping between nearest-neighbor sites and $\epsilon_i$'s in the second term are the random on-site potential uniformly distributed in the interval $[-W/2, W/2]$. In eq. (1), the energy $t$ is associated with nearest neighbor hopping integral, which is about 2.7 eV in graphene. This model has recently been studied by transfer-matrix method in ref. [18], where it was found that all states are localized, in agreement with scaling theory of localization in 2D. However, our results are in contradiction with this finding.

In our work, to investigate the localization properties, we employ the so-called *typical DOS* as a quantity which determines whether a given state with energy $E$ is extended or localized [16]. The return probability for an extended state at a given energy $E$ is zero [19]. Therefore the self-energy of an extended state acquires an imaginary part to account for the decay of return probability, while the self-energy for localized states remains purely real. This reflects itself in the local density of states (LDOS):

$$\rho_s(E) = \sum_k |\langle s|E_k\rangle|^2 \delta(E - E_k), \tag{2}$$

where $|s\rangle$ denotes a localized basis state at site $s$, while $|E_k\rangle$ is an energy eigen-vector corresponding to energy $E_k$. Examining LDOS at $K_s$ sites provides a measure to distinguish localized states from extended ones. To do so, one defines the typical DOS which is a geometrical average of LDOS's,

$$\rho_{\text{typ}}(E) = \exp\left[\frac{1}{K_r K_s} \sum_r^{K_r} \sum_s^{K_s} \ln\left(\rho_s^r(E)\right)\right], \tag{3}$$

where $K_r$ is the number of realizations used in numerical calculations. We also need the total spectral weight which can be obtained from the following arithmetic averaging:

$$\rho(E) = \frac{1}{K_r K_s} \sum_r^{K_r} \sum_s^{K_s} \rho_s^r(E) = \frac{1}{D} \sum_{k=0}^{D-1} \delta(E - E_k), \tag{4}$$

where $D$ is the dimension of the Hilbert space on which the Hamiltonian $H$ is acting.

The core quantity in both eqs. (3) and (4) is the LDOS. In order to calculate quantities of this sort, the KPM method [16] employs a complete basis set.

The basic idea behind the KPM is to expand the spectral function, say, $\rho_s(E)$, in terms of orthogonal polynomials, $\phi_m(E)$, In general, all types of orthogonal polynomials can be used. In the case of, *e.g.*, Chebyshev polynomials one has

$$\rho_s(E) = \frac{1}{\pi\sqrt{1-E^2}} \left[\mu_0 + 2\sum_{m=1}^{M} \mu_m T_m(E)\right], \tag{5}$$

where

$$\mu_m = \int_{-1}^{1} \rho_s(E) T_m(E) \mathrm{d}E = \frac{1}{D} \langle s|T_m(\tilde{H})|s\rangle. \tag{6}$$

Here, $\tilde{H}$ is obtained from $H$ by a simple linear transformation to ensure that the eigenvalues of $\tilde{H}$ are in $[-1, 1]$. The same procedure when applied to eq. (4) gives

$$\mu_m = \int_{-1}^{1} \rho(E) T_m(E) \mathrm{d}E = \frac{1}{D} \mathrm{Tr}[T_m(\tilde{H})]. \tag{7}$$

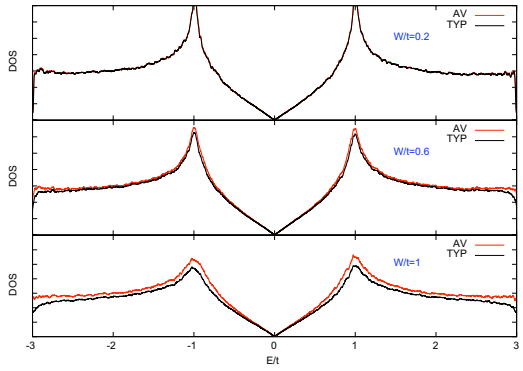


Fig. 1: (Color online) $\rho$ (solid line) and $\rho_{\rm typ}$ (dotted line) for different values of disorder strength $W$ in the weak-disorder regime ($W \lesssim t$). In this regime the disorder only renormalizes the Fermi velocity of Dirac quasi-particles. Our results are stable with respect to change in both lattice size, as well as $M$.

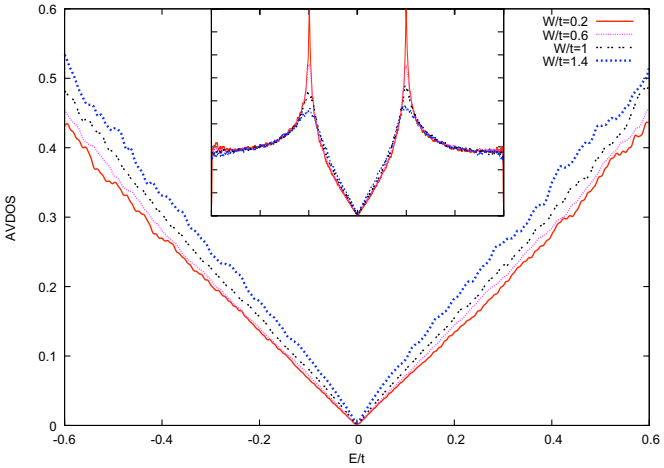


Fig. 2: (Color online) Average DOS as a function of energy. By increasing $W$ in weakly disordered region, the velocity of Dirac fermions decreases.

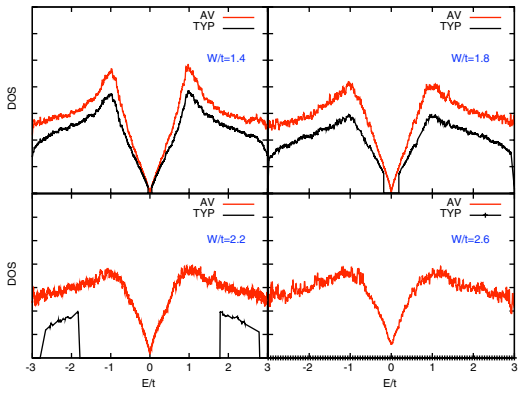


Fig. 3: (Color online) For $W > t$ a mobility edge starts to appear. $\rho_{\rm typ}$ is zero around the Fermi energy. Therefore localized states fall into a "gap" separating extended states of the valance and conduction bands.

Equations (7) and (6) can be evaluated with a recursive relation first discussed by Wang [20]. The Tr in eq. (7) can be most conveniently evaluated with a simple stochastic summation employing the recursion relation among Chebyshev polynomials [16]. However, since $M$ in eq. (5) is finite in computer implementations, one faces the classic problem of Gibbs oscillations. There are standard attenuation factors suggested in the literature which minimize such unwanted oscillations [16,20]. Due to peculiar Dirac dispersion in graphene, none of the so-called $g$-factors worked. The solution around this problem is to use regulated (Gaussian broadened) polynomials to calculate the moments [17]:

$$\langle \phi_m(x) \rangle_\sigma \equiv \frac{1}{2\pi\sigma^2} \int {\rm d}x' e^{-(x'-x)^2/2\sigma^2} \phi_m(x'). \qquad (8)$$

Our present calculation is based on using Legendre polynomials in (8) with $\sigma$ equal to $4/M$.

**Results and discussions.** – To investigate the Anderson transition in graphene, we use eq. (1) with different values of $W$ and then calculate the LDOS via the RKPM method with $M$ equal to 5000–12000 on a lattice with $10^6$ sites. The result for different values of $W$ is shown in fig. 1. As can be seen in fig. 1 the average DOS for various values of $W \lesssim t$ resembles that of perfect graphene. The typical DOS, $\rho_{\rm typ}$, is non-zero everywhere, indicating that none of the states are localized in this regime. The role of disorder at weakly disordered regime is to slow down the Dirac quasi-particles, with their Dirac nature preserved. This result is in agreement with other works [21,22]. Figure 2 shows the renormalization of the Dirac fermion's velocity. By increasing the disorder strength, the slope of $\rho$ decreases. Therefore, according to $\rho(\omega) \propto |\omega|/v_F^2$, the velocity of quasi-particles decreases when $W$ increases [15,21].

Increasing $W$ to the strong-disorder regime, $W \gtrsim t$, we observe a mobility edge in graphene in fig. 3. The mobility edge starts at the Fermi energy and keeps moving to both the left and right side separating localized states around Fermi energy from those at higher energies. This is unlike the usual scenario of localization where states at the band edge start to localize first.

The idea of band gap opening in graphene has already been proposed by several groups. Pereira *et al.* [23] by selectively producing vacant sites in only one sub-lattice, found the appearance of a clean gap without any states in it. Substrate-induced band gap, which is accompanied by breaking the particle-hole symmetry is another possible scenario [24].

However, our result suggest the possibility of *disorder-induced gap* in graphene. This gap is defined as the distance between the upper and lower mobility edges around the Fermi point of graphene. We find that in the intermediate disorder regime ($W \sim t$) states at the

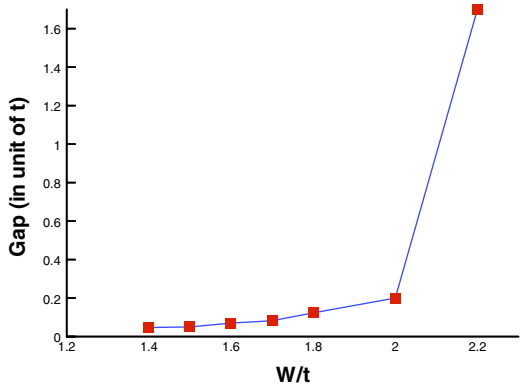


Fig. 4: (Color online) Gap (distance between the mobility edges around the neutrality point) *vs.* disorder strength.

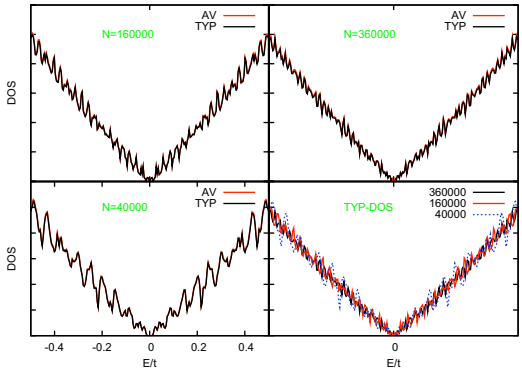


Fig. 5: (Color online) Size dependence of typical and average DOS for states near the Dirac point.

Fermi point start to localize, thereby opening a small gap around it (fig. 3). The states inside the gap are localized and cannot contribute in transport phenomena. Upon increasing disorder strength, this gap rises slowly up to $W \sim 2t$, above which its growth speeds up with a high slope (fig. 4). This behavior can be assigned to cross-over from weak to strong localization regimes. Naumis also obtains such disorder-induced gap, using a real space renormalization group scheme [25] for vacancy-doped graphene. Nevertheless this gap continuously grows from zero as a function of doping ratio.

Finally with increasing $W$ beyond $W_c/t = 2.5 \pm 0.5$, all states in the band become localized. The "error" $\pm 0.5$ here needs clarification: One might argue that the typical DOS is not the best quantity to distinguish localized states from extended ones. Our benchmark runs for the known results of the critical $W$ for the 3D cubic systems gives $W_c^{3D}/t = 16.0 \pm 0.5$. Therefore the possible intrinsic error in finding $W_c$ in this method is less than 0.5.

**Conclusion.** – For the Anderson model, in weak-disorder regime, we observe that the Dirac fermions remain delocalized up to $W^* \approx t$. In this regime, the effect of disorder is to decrease the velocity of Dirac fermions, hence resulting in a renormalized Dirac cone. However, upon increasing the disorder strength beyond $W^*$ in this model, we observe a mobility edge, in agreement with ref. [25]. Our results support the idea proposed by Suzuura and Ando [26] which explains the suppression of weak localization in graphene. According to their argument, the change in relative weights of the two components of chiral electrons wave functions induces a new Berry phase, when these electrons move along a closed path. If the inter-valley scatterings are negligible, this new phase changes the sign of the wave function in a given path with respect to its time-reversed counterpart, leading to a destructive interference of the two paths, hence leaving the low-energy sates extended. A similar result has also been obtained in recent theoretical work on chemiabsorbed adatoms attached to the carbon atoms in graphene [27]. Another single-impurity study using the scattering formulation indicates the possibility of localization due to bound-state formation for strong enough scattering strength [28]. Although our method is not able to estimate the contributions of inter-valley and intra-valley scatterings separately, we speculate that the relative intensity of inter-valley scattering might be small. We think the localization of all the electronic states, obtained by transfer matrix method [18], might be due to size limitations, which makes their method inconclusive in the weak-disorder limit ($W/t < 1$). We have performed a careful finite-size scaling specially in the weak-disorder regime. Figure 5 shows the finite-size analysis at $W/t = 0.3$ for the lattice sizes $N = 4 \times 10^4$, $16 \times 10^4$, $36 \times 10^4$ near the Dirac point. As can be seen in the figure, the typical DOS remains non-zero as one increases the lattice size. This clearly means that states near the Dirac point remain extended in the weak-disorder regime. It should be noted that the number of moments, $M$ used in the polynomial expansion must be large enough ($M \propto N^1$). Upon increasing the disorder strength, when it becomes comparable with the hopping energy ($W \sim t$), the inter-valley scatterings get significant and the weak localization will be eventually recovered around the Fermi points [29–32]. In the very strong-disorder regime ($W > 2t$), localization quickly spreads over all the energy spectrum. In this case the system is no longer homogeneous in the sense that it divides into regions with different chemical potential and transport is described in terms of percolation in the real space [33,34]. A recent study employing the same method as ours on graphene nano-ribbons agrees with our results [35].

Some aspects of our predictions are qualitatively verified in the recent ARPES measurements of graphene samples dosed with atomic hydrogen [36]: i) The very observation of metal-insulator transition at finite amount of short-range disorder due to adsorbed hydrogen atoms. ii) The observed gap is due to the emergence of a mobility edge around the charge neutrality point in agreement with our work and ref. [25].

* * *

FS and SAJ thank the Abdus Salam ICTP for the hospitality during a short-term summer visit, where some part of this work was done. This work was partially supported by ALAVI Group Ltd. We are also indebted to S. Sota, R. Asgari and F. Fazileh for useful discussions.

REFERENCES

[1] Novoselov K. S. *et al.*, *Science*, **306** (2004) 666.
[2] Novoselov K. S. *et al.*, *Nature*, **438** (2005) 197.
[3] Geim A. K. and Novoselov K. S., *Nat. Mater.*, **6** (2007) 183.
[4] Land T. A., Michely T., Behm R. J., Hemminger C. J. and Comsa G., *Surf. Sci.*, **264** (1992) 261; Nagashima A. *et al.*, *Surf. Sci.*, **291** (1993) 93.
[5] Berger C. *et al.*, *J. Phys. Chem. B*, **108** (2004) 19912; *Science*, **312** (2006) 1191.
[6] Castro Neto A. H., Guinea F., Peres N. M. R., Novoselov K. S. and Geim A. K., *Rev. Mod. Phys.*, **81** (2009) 109.
[7] Wallace P. R., *Phys. Rev.*, **71** (1947) 622.
[8] Semenof G. W., *Phys. Rev. Lett.*, **53** (1984) 2449.
[9] Abrahams E., Anderson P. W., Licciardello D. C. and Ramakrishnan T. V., *Phys. Rev. Lett.*, **42** (1979) 673.
[10] Lee P. A. and Ramakrishnan T. V., *Rev. Mod. Phys.*, **57** (1985) 287.
[11] Ostrovsky P. M., Gornyi I. V. and Mirlin A. D., *Phys. Rev. Lett.*, **98** (2007) 256801.
[12] Bardarson J. H., Tworzydlo J., Brouwer P. W. and Beenakker C. W. J., *Phys. Rev. Lett.*, **99** (2007) 106801.
[13] Nomura K., Koshino M. and Ryu S., *Phys. Rev. Lett.*, **99** (2007) 146806.
[14] Abedpour N. *et al.*, *Phys. Rev. B*, **76** (2007) 195407.
[15] Lherbier A. *et al.*, *Phy. Rev. Lett.*, **100** (2008) 036803; Triozon F. *et al.*, *Phys. Rev. B*, **69** (2004) 121410.
[16] Weisse A. *et al.*, *Rev. Mod. Phys.*, **78** (2006) 275.
[17] Sota Shigetoshi and Itoh Masaki, *J. Phys. Soc. Jpn.*, **76** (2007) 054004.
[18] Xiong S. J. and Xiong Y., *Phys. Rev. B*, **76** (2007) 214204.
[19] Philips P., *Advanced Solid State Physics*, 1st edition (Westview Press) 2002.
[20] Wang Lin-Wang, *Phys. Rev. B*, **49** (1994) 10154.
[21] Hu B. Yu-Kuang, Hwang E. H. and Das Sarma S., *Phys. Rev. B*, **78** (2008) 165411.
[22] Qaiumzadeh A., Arabchi N. and Asgari R., *Solid State Commun.*, **147** (2008) 172.
[23] Pereira Vitor M., Lopes dos Santos J. M. B. and Castro Neto A. H., *Phys. Rev. B*, **77** (2008) 115109.
[24] Zhou S. Y. *et al.*, *Nat. Mater.*, **6** (2007) 770; **7** (2008) 259.
[25] Naumis G. G., *Phys. Rev. B*, **76** (2007) 153403.
[26] Suzuura H. and Ando T., *Phys. Rev. Lett.*, **89** (2002) 266603.
[27] Robinson J. P., Schomerus H., Oroszlany L. and Fal'ko V. I., *Phys. Rev. Lett.*, **101** (2008) 196803.
[28] Basko D. M., *Phys. Rev. B*, **78** (2008) 115432.
[29] Altland A., *Phys. Rev. Lett.*, **97** (2006) 236802.
[30] Aleiner I. L. and Efetov K. B., *Phys. Rev. Lett.*, **97** (2006) 236801.
[31] Louis E. J., Vergés A., Guinea F. and Chiappe G., *Phys. Rev. B*, **75** (2007) 085440.
[32] McCann E. *et al.*, *Phys. Rev. Lett.*, **97** (2006) 146805; Kechedzhi K. *et al.*, *Eur. Phys. J. ST*, **148** (2007) 3954.
[33] Cheianov V. V., Fal'ko V. I., Altshuler B. L. and Aleiner I. L., *Phys. Rev. Lett.*, **99** (2007) 176801.
[34] Shklovskii B. I., *Phys. Rev. B*, **76** (2007) 233411.
[35] Schubert G., Schleede J. and Fehske H., *Phys. Rev. B*, **79** (2009) 235116.
[36] Bostwick A., McChesney J. L., Emstev K., Seyller T., Horn K., Kevan S. D. and Rotenberg E., arXiv:0904.2249v1 (2009).

# STOCHASTIC SENSITIVITY AND TRANSITION TO CHAOS

**IRINA BASHKIRTSEVA**

We suggest a new technique for analysis of the forced nonlinear oscillations based on stochastic sensitivity function (SSF). This function describes the dispersion of random trajectories near deterministic attractor. The possibilities of SSF to predict some peculiarities of dynamics for stochastically and periodically forced oscillators are shown. The thin effects observed in Brusselator, stochastic Lorenz and Chen models near chaos in a period-doubling bifurcations zone are presented. The problem of noise-induced transitions from order to chaos for stochastic cycles is considered.

# Chaos from turbulence: stochastic-chaotic equilibrium in turbulent convection

A. Bershadskii
*ICAR, P.O.B. 31155, Jerusalem 91000, Israel*

It is shown that correlation function of the mean wind velocity generated by a turbulent thermal convection (Rayleigh number $Ra \sim 10^{11}$) exhibits exponential decay with a very long correlation time, while corresponding largest Lyapunov exponent is certainly positive. These results together with the reconstructed phase portrait indicate presence of chaotic component in the examined mean wind. Relative contribution of the chaotic and stochastic components to the mean wind fluctuations and an equilibrium between these components has been studied in detail. An analogy with quantum chaos has been also discussed.

**Advanced Workshop on**
**"Anderson Localization, Nonlinearity and Turbulence: A Cross-Fertilization"**

**ICTP, Trieste, Italy, 23 August - 3 September 2010**

**Joshua BODYFELT**
MPI-PKS
Dresden, Germany

**TITLE:**
**``One Parameter Scaling Theory for Stationary States of Disordered Nonlinear Systems"**

ABSTRACT:

We show, using detailed numerical analysis and theoretical arguments, that the normalized participation number of the stationary solutions of disordered nonlinear lattices obeys a one-parameter scaling law. Our approach opens a new way to investigate the interplay of Anderson localization and nonlinearity based on the powerful ideas of scaling theory.

# Localization-Delocalization Transition through Graphene Superlattice with Long-Range Correlated Disorder on Potential Barriers

***Hosein Cheraghchi*[1], *Amir Hossein Irani*[1], *Seyyed Mahdi Fazeli*[2]**
[1]*Department of Physics, Damghan University of Basic Sciences, Damghan, Iran*
[2]*Department of Physics, Ghom University, Ghom, Iran*

## Abstract:

Using transfer matrix method, we have solved Dirac equation for chiral particles in graphene supperlattice with long-range correlated disorder on potential barriers. Long range correlated random data is produced by the mid-point method. Because of Klein tunneling, electrons with normal incident can transport without any reflection. The same phenomenon is seen when transmission through disordered superlattices is calculated. But in large angles incidence to the potential barriers, transmission is suppressed by uncorrelated disorder. However, transport is allowed in wide range of angles when the potential heights are correlated with the correlation strength H (named by the Hurst exponent). As a result, conductance increases with the Hurst exponent. We have provided a phase transition diagram in which critical Hurst exponent depends on the disorder strength. It is also investigated the dependence of conductance to the width and length of the barriers. Energy range of this study has chosen in such way that transport is in its propagating modes.

# Turbulent Square-Root Broadening of Fiber Lasers Output Spectrum

**S.A. Babin, D.V. Churkin, A.E. Ismagulov, S.I. Kablukov, E.V. Podivilov**

*Institute of Automation and Electrometry, Novosibirsk, Russia; e-mail: churkin@iae.nsk.su*

## Motivation

- Fiber laser output spectrum is usually broadened because of nonlinear effects.
- Exact mechanism is unknown as well as there is not a general theoretical description.
- Thus, the output power, spectral shape and width can not be calculated.
- An approach of weak wave turbulence can describe the spectrum of one type of fiber laser - Raman fiber laser - in the case of high-Q cavity [1,2]. Is it possible to describe the output characteristics of the conventional RFL of low-Q cavity?

## Long Raman fiber laser

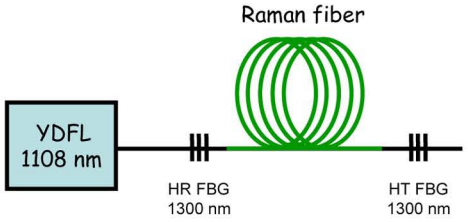


## Analytical theory: wave turbulence in a fiber

Stokes wave spectrum

Effective FBGs losses — Raman gain

$$\left(\delta(\Omega)+2\alpha L+\delta_{NL}\right)I(\Omega)=2g_R L\bar{P}I(\Omega)+\frac{\delta_{NL}}{I^2}\int I(\Omega_1)I(\Omega_2)I(\Omega_1+\Omega_2-\Omega)d\Omega_1 d\Omega_2$$

Nonlinear FWM-induced homogeneous losses: Stokes wave mode ($\Omega$) scatters to others.

$$\delta_{NL}=K\gamma IL$$

Nonlinear FWM-induced inhomogeneous gain: Stokes wave modes ($\Omega_1$) and ($\Omega_2$) scatters to the Stokes wave mode ($\Omega$).

V. Zakharov et al., Springer, 1992

## Fiber laser output spectrum and power: analytical solution

### RFL output power

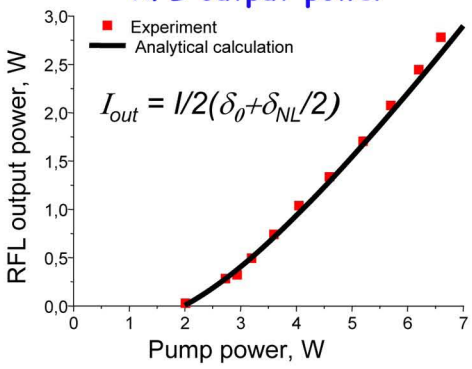


### RFL output spectrum

$$I_{out}(\Omega)=\frac{I}{2}\pi\Omega\sqrt{\frac{\delta_2}{2\delta_{NL}}}\frac{\delta_0+\delta_2\Omega^2}{\cosh\left(\pi\Omega\sqrt{\frac{\delta_2}{2\delta_{NL}}}\right)}$$

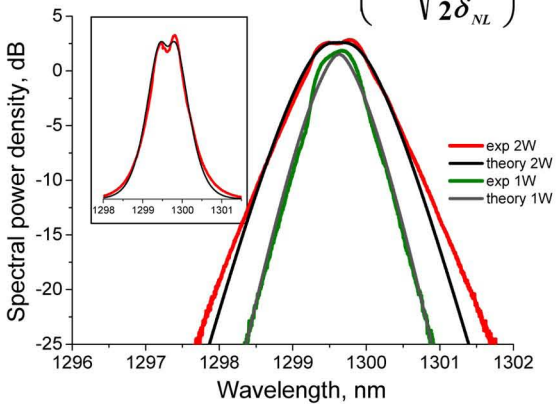


### RFL output spectral width

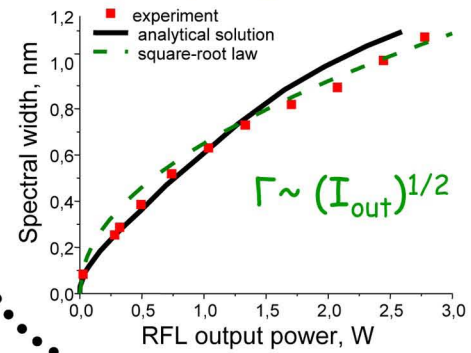


The wave turbulence approach predicts well RFL output spectrum, output power and output spectrum width thus enabling easy laser optimization.

TO READ:

1. S. A. Babin et al., "Spectral broadening in Raman fiber lasers", Opt. Lett. 31(20), 3007, 2006.
2. S. A. Babin et al., "FWM-induced turbulent spectral broadening in a long Raman fiber laser", JOSA B, 24(8), 1729, 2007.

Turbulent ratchet transport of interacting particles

We study the ratchet transport of interacting particles induced by a monochromatic driving in asymmetric two-dimensional structures in the presence of a constant transversal magnetic field.

The complex behavior of the system is analyzed for different values of polarized electrical field and the rest of the parameters of the problem.

The numerical data show emergence of turbulence in the ratchet ï¬‚ow under certain conditions.

Finally, the magnetic field symmetries are studied for different interaction strenght between particles.

# Real-Space Renormalization Group for Anderson Localization of Interacting Electrons in the Anderson-Hubbard Model

Roman Katzer, Peter Henseler, and Johann Kroha
Physikalisches Institut, Universität Bonn, Germany

Anderson localization of interacting fermions remains a controversial issue even for short-range interaction. We construct a real-space renormalization group (RG) approach for the disordered Hubbard model with random onsite single-particle energies $\varepsilon_i$. The Hubbard interaction $U$ leads to a non-trivial random distribution of many-body energy levels. In the atomic limit (hopping $t \to 0$ adiabatically, while keeping the chemical potential equal on all sites) this distribution can be calculated exactly, depending on $\varepsilon_i$, $U$ and the filling fraction, and can be expressed in terms of a modified ("screened") single-particle level distribution [1]. Switching on hopping ($t \neq 0$), successively increasing the real-space cluster size and mapping a cluster onto a single site generates an RG flow in the space of disordered many-body Hamiltonians. Restricting the flow to low energies and observing the spin structure, the Fock space may be decimated in each RG step to keep only three Fock-space sectors with consecutive cluster occupation numbers and in each sector the lowest energy state. This leads to an RG flow of disordered Hubbard models, where the flow of the random distribution of energy levels serves as indicator for localization or delocalization. The evaluation of this scheme in $d = 1$ agrees with previous results.

[1] P. Henseler, J. Kroha and B. Shapiro, Phys. Rev. B **77**, 075101 (2008); **78**, 235116 (2008).

# Interaction induced fractional Bloch and tunneling oscillations

Ramaz Khomeriki[1,2] Dmitry O. Krimer[1], Masudul Haque[1] and Sergej Flach[1]
[1] *Max-Planck Institute for the Physics of Complex Systems, Nöthnitzer Str. 38, 01187 Dresden, Germany*
[2] *Physics Department, Tbilisi State University, Chavchavadze 3, 0128 Tbilisi, Georgia*

We study the dynamics of few interacting bosons in a one-dimensional lattice with dc bias. In the absence of interactions the system displays single particle Bloch oscillations. For strong interaction the Bloch oscillation regime reemerges with fractional Bloch periods which are inversely proportional to the number of bosons clustered into a bound state. The interaction strength is affecting the oscillation amplitude. Excellent agreement is found between numerical data and a composite particle dynamics approach. For specific values of the interaction strength a particle will tunnel from the interacting cloud to a well defined distant lattice location.

PACS numbers: 67.85.-d, 37.10.Jk, 03.65.Ge

Bloch oscillations [1] in dc biased lattices are due to wave interference and have been observed in a number of quite different physical systems: atomic oscillations in Bose-Einstein Condensates (BEC) [2], light intensity oscillations in waveguide arrays [3], and acoustic waves in layered and elastic structures [4], among others.

Quantum many body interactions can alter the above outcome. A mean field treatment will make the wave equations nonlinear and typically nonintegrable. For instance, for many atoms in a Bose-Einstein condensate, a mean field treatment leads to the Gross-Pitaevsky equation for nonlinear waves. The main effect of nonlinearity is to deteriorate Bloch oscillations, as recently studied experimentally [5] and theoretically [6–8].

In contrast, we will explore the fate of Bloch oscillations for quantum interacting few-body systems. This is motivated by recent experimental advance [9] in monitoring and manipulating few bosons in optical lattices. Few body quantum systems are expected to have finite eigenvalue spacings, consequent quasiperiodic temporal evolution and phase coherence. In a recent report on interacting electron dynamics spectral evidence for a Bloch frequency doubling was reported [10]. On the other hand, it has been also recently argued that Bloch oscillations will be effectively destroyed for few interacting bosons [11].

In the present paper we show that for strongly interacting bosons a coherent Bloch oscillation regime reemerges. If the bosons are clustered into an interacting cloud at time $t = 0$, the period of Bloch oscillations will be a fraction of the period of the noninteracting case, scaling as the inverse number of interacting particles (Fig.1). The amplitude (spatial extent) of these fractional Bloch oscillations will decrease with increasing interaction strength. For specific values of the interaction, one of the particles will leave the interacting cloud and tunnel to a possibly distant and well defined site of the lattice. For few particles the dynamics is always quasiperiodic, and a decoherence similar to the case of a mean field nonlinear equation [7] will not take place.

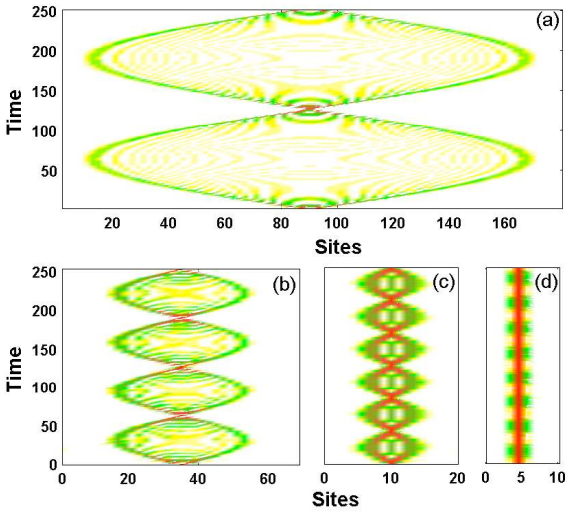


FIG. 1: Time evolution of the probability density function (PDF) $P_j(t)$ for the interaction constant $U = 3$ and dc field $E = 0.05$ and different particle numbers initially occupying a single site at $t = 0$. (a) shows one particle Bloch oscillations with the conventional Bloch period $2\pi/E$, while (b), (c) and (d) display two, three and four particle oscillations with the periods $2\pi/(2E)$, $2\pi/(3E)$ and $2\pi/(4E)$, respectively.

We consider the Bose-Hubbard model with a dc field:

$$\hat{\mathcal{H}} = \sum_j \left[ t_1 \left( \hat{b}^+_{j+1}\hat{b}_j + \hat{b}^+_j \hat{b}_{j+1} \right) + Ej\hat{b}^+_j\hat{b}_j + \frac{U}{2}\hat{b}^+_j\hat{b}^+_j\hat{b}_j\hat{b}_j \right] \tag{1}$$

where $\hat{b}^+_j$ and $\hat{b}_j$ are standard boson creation and annihilation operators at lattice site $j$; the hopping $t_1 = 1$; $U$ and $E$ are the interaction and dc field strengths, respectively. To study the dynamics of $n$ particles we use the orthonormal basis of states $|\mathbf{k}\rangle \equiv |k_1, k_2, ..., k_n\rangle = b^+_{k_1} b^+_{k_2} ... b^+_{k_n} |0\rangle$ where $|0\rangle$ is the zero particle vacuum state, and $k_1 \leq k_2 ... \leq k_n$ are lattice site indices (for instance, in the case of two particles the state representation is mapped to the triangle). The eigenvectors $|\nu\rangle$ of Hamil-

tonian (1) with eigenvalues $\lambda_\nu$ are then given by:

$$|\nu\rangle = \sum_{\mathbf{k}} A^\nu_{\mathbf{k}} |\mathbf{k}\rangle \ , \qquad \hat{\mathcal{H}}|\nu\rangle = \lambda_\nu |\nu\rangle \tag{2}$$

where the eigenvectors $A^\nu_{\mathbf{k}} \equiv \langle \mathbf{k}|\nu\rangle$ and the time evolution of a wave function $|\Psi(t)\rangle$ is given by

$$|\Psi(t)\rangle = \sum_\nu \Phi_\nu e^{-i\lambda_\nu t}|\nu\rangle, \qquad \Phi_\nu \equiv \langle \nu|\Psi(0)\rangle. \tag{3}$$

We monitor the probability density function (PDF) $P_j(t) = \langle\Psi(t)|\hat{b}^+_j\hat{b}_j|\Psi(t)\rangle/n$, which can be also computed using the eigenvectors and eigenvalues:

$$P_j(t) = \frac{1}{n}\sum_{\nu,\mu} \Phi_\nu \Phi^*_\mu e^{i(\lambda_\mu - \lambda_\nu)t}\langle\mu|\hat{b}^+_j\hat{b}_j|\nu\rangle \ . \tag{4}$$

In Fig.1 we show the evolution of $P_j(t)$ for $U = 3$, $E = 0.05$ and $n = 1, 2, 3, 4$ with initial state $k_1 = k_2 = ... = k_n \equiv p$, i.e. when all particles are launched on the same lattice site $p$. For $n = 1$ we observe the usual Bloch oscillations with period $T = 2\pi/E$ (Fig.1(a) and below). Due to the small value of $E$, the amplitudes of oscillations are large. However, with increasing number of particles, we find that the oscillation period is reduced according to $2\pi/(nE)$, and at the same time the amplitude of oscillations is also reduced.

*One particle case:* For $n = 1$ the interaction term in (1) does not contribute. The eigenvalues $\lambda_\nu = E\nu$ (with $\nu$ being an integer) form an equidistant spectrum which extends over the whole real axis - the Wannier-Stark ladder. The corresponding eigenfunctions obey the generalized translational invariance $A^{\nu+\mu}_{k+\mu} = A^\nu_k$ [1] and are given by the Bessel function $J_k(x)$ of the first kind [12, 13]

$$A^\nu_k = J^\nu_k \equiv J_{k-\nu}(2/E). \tag{5}$$

All eigenvectors are spatially localized with an asymptotic decay $|A^0_{k\to\infty}| \to (1/E)^k/k!$, giving rise to the well-known localized Bloch oscillations with period $T_B = 2\pi/E$. The localization volume $\mathcal{L}$ of a single particle eigenstate characterizes its spatial extent. It follows $\mathcal{L} \propto -[E\cdot \ln E]^{-1}$ for $E \to 0$ and $\mathcal{L} \to 1$ for $E \to \infty$ [7]. For $E = 0.05$ the single particle oscillates with amplitude of the order of $2\mathcal{L} \approx 160$ (Fig.1(a)). According to Eqs. (4) and (5) the probability density function is given by:

$$P_j(t) = \sum_{\nu,\mu} J^\nu_p J^\mu_p J^\nu_j J^\mu_j e^{iE(\mu-\nu)t}. \tag{6}$$

*Two particle case (n=2):* For $U = 0$ the eigenfunctions of the Hamiltonian (1) are given by tensor products of the single particle eigenstates:

$$|\mu,\nu\rangle = \sqrt{\frac{2-\delta_{\mu,\nu}}{2}}\sum_{k,j} J^\mu_k J^\nu_j \hat{b}^+_k\hat{b}^+_j|0\rangle \ , \ \mu \le \nu \ . \tag{7}$$

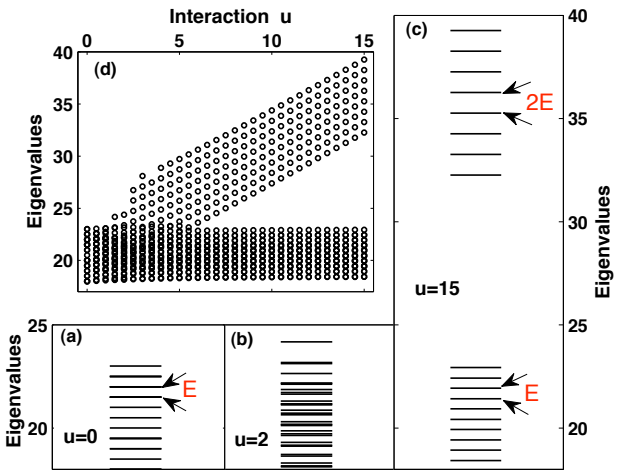


FIG. 2: Eigenvalue spectrum for $n = 2$, $E = 0.5$ and different interaction constants $U$. The eigenvalues are displayed only for eigenvectors localized in the center of the lattice (we select the 32 eigenstates which overlap most strongly with the center of the lattice) (a): $U = 0$, the spectrum is equidistant with spacing $E$ and degenerate. (b): $U = 2$, the degeneracy is lifted. (c): $U = 15$, the spectrum decomposes into two subspectra, with two different equidistant spacings - $E$ and $2E$. Graph (d) displays the eigenvalue spectrum of the 32 central eigenfunctions as a function of $U$.

The corresponding eigenvalues form an equidistant spectrum which is highly degenerate:

$$\hat{\mathcal{H}}|\mu,\nu\rangle = (\mu+\nu)E|\mu,\nu\rangle \tag{8}$$

For the above initial condition $k_1 = k_2 \equiv p$ the expression for the PDF (6) is still valid (actually it is for any number of noninteracting particles), with the same period $2\pi/E$ of Bloch oscillations as in the single particle case.

For nonvanishing interaction the degeneracy of the spectrum is lifted, and the eigenvalues of overlapping states are not equidistant any more (Fig.2). Therefore we observe quasiperiodic oscillations which however are still localizing the particles. For even larger values of $U$ the basis states with two particles on the same site will shift their energies by $U$ exceeding the hopping $2t_1$. Therefore for $U > 2t_1$ the spectrum will be decomposed into two nonoverlapping parts - a noninteracting one which excludes double occupancy and has equidistant spacing $E$, and an interacting part which is characterized by almost complete double occupancy and has corresponding equidistant spacing $2E$, which is the cost of moving two particles from a given site to a neighboring site. Some initial state can overlap strongly with eigenstates from one or the other part of the spectrum, and therefore result in different Bloch periods. In particular, when launching both particles on the same site, one strongly overlaps with the interacting part of the spectrum and observes a fractional Bloch period $2\pi/(2E)$.

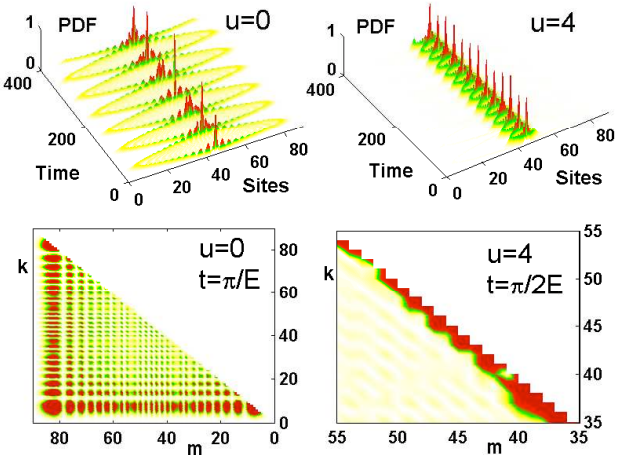


FIG. 3: Upper plots: PDF for $E = 0.1$, $n = 2$, single site initial occupancy and different interaction constants. For $U = 0$ we find single particle Bloch oscillations. For $U = 4$ fractional Bloch oscillations take place, in agreement with (11). Lower plots: probability density of the evolved wave function (darker regions correspond to larger probablilities) after one half of the respective Bloch period. For $U = 0$ the two particles are with equal probability close to each other and at maximal separation. For $U = 4$ the two particles avoid separation and form a composite particle which coherently oscillates in the lattice. In lower graphs we use triangle $k < m$ mapping for indistinguishable two particle state representation (index $m$ increases from the right to the left).

In order to calculate the amplitude of these fractional Bloch oscillations, we note that for $E = 0$ there exists a two-particle bound state band of extended states with band width $\sqrt{U^2+16} - U$ [14]. For large $U$ the bound states are again almost completely described by double occupancy. Therefore we can construct an effective Hamiltonian for a composite particle of two bound bosons:

$$\hat{\mathcal{H}} \approx \sum_j \left[ t_2 \left( \hat{R}^+_{j+1} \hat{R}_j + \hat{R}^+_j \hat{R}_{j+1} \right) + 2Ej \hat{R}^+_j \hat{R}_j \right] \quad (9)$$

where $\hat{R}^+_j$ and $\hat{R}_j$ are creation and annihilation operators at lattice site $j$ of the composite particle (two bosons on the same site) with the effective hopping

$$t_2 = \frac{\sqrt{U^2+16} - U}{4}. \quad (10)$$

The corresponding PDF is given by

$$P_j(t) = \sum_{\nu,\mu} A^\nu_p A^\mu_p A^\nu_j A^\mu_j e^{i2E(\mu-\nu)t} . \quad (11)$$

The composite particle eigenvectors $A^\nu_p = J_{\nu-p}(2t_2/(2E))$ are again expressed through Bessel functions, but with a modified argument as compared to the single particle case. Bloch oscillations will evolve with fractional period $2\pi/(2E)$ as observed in Fig.1(b). The amplitude of the oscillations is reduced with increasing $U$ since the hopping constant $t_2$ is reduced (Fig.3). For $U = 3$ it follows $t_2 = 0.5$, and together with the doubled Bloch frequency the localization volume should be reduced by a factor of 4 as compared to the single particle case. This is precisely what we find when comparing Fig.1(a,b): for $n$=1 the amplitude is 160 sites, while for $n = 2$ it is 40 sites. In the lower plots in Fig.3 we show the probability density of the wave functions $|\langle\Psi(t)|\mathbf{k}\rangle|^2$ after one half of the respective Bloch period in the space of the two particle coordinates with $k_1 = k$ and $k_2 = m$. For $U = 0$ both particles are with high probability at a large distance from each other. Therefore the density is large not only for $k = m$ (the two particles are at the same site), but also for $k = 5$, $m = 85$ (the two particles are at maximum distance). However, for $U = 4$ we find that the two particles, which initially occupy the site $p = 45$, do not separate, and the density is large only along the diagonal $k = m$ with $35 \le k \le 55$. (For $U = 4$, the localization volume is $\sim 20$.) Therefore, the two particles indeed form a composite state and travel together.

*$n$ particle case:* We proceed similar to the case $n = 2$ and estimate perturbatively the effective hopping constant for a composite particle of $n$ bosons. For that we use the calculated width of the $n$-particle bound state band for $E = 0$ [14]. In leading order of $1/U$ it reads [14]:

$$t_n \simeq \frac{n}{U^{n-1}(n-1)!}. \quad (12)$$

For $n = 2$ the above expression gives $t_2 \simeq 2/U$, the first expansion term of the exact relation for two bosons (10). The corresponding composite particle Hamiltonian

$$\hat{\mathcal{H}} \approx \sum_j \left[ t_n \left( \hat{R}^+_{j+1} \hat{R}_j + \hat{R}^+_j \hat{R}_{j+1} \right) + nEj \hat{R}^+_j \hat{R}_j \right] . \quad (13)$$

The PDF is given by

$$P_j(t) = \sum_{\nu,\mu} A^\nu_p A^\mu_p A^\nu_j A^\mu_j e^{inE(\mu-\nu)t} , \quad (14)$$

and the composite particle eigenvectors $A^\nu_p = J_{\nu-p}(2t_n/(nE))$. Bloch oscillations will evolve with fractional period $2\pi/(nE)$ as observed in Fig.1(c,d). The amplitude of the oscillations is reduced with increasing $U$ since the hopping constant $t_n$ is reduced. For $U = 3$ and $n = 3$ it follows $t_3 = 0.17$, and for $n = 4$ we have $t_4 = 0.01$. This leads to a reduction factor 18 and 400 respectively as compared to the single particle amplitude and yields amplitudes of the order of 9 and 0.5 respectively, which is in good agreement with the numerically observed amplitudes (10 and 2 sites respectively) in Fig.1(c,d).

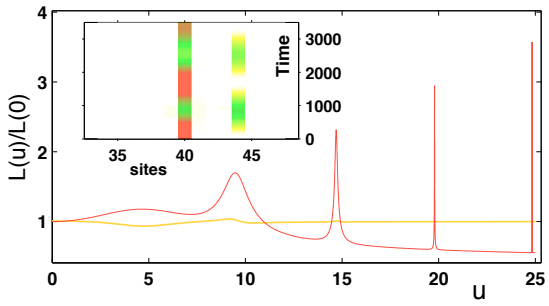


FIG. 4: Time averaged and normalized localization volume $L$ of the wavepacket which emerge from two initial distributions as a function of $U$ for $E = 5$. Red (grey) curve: two particles are launched on the same site. Orange (light grey) curve: two particles are launched on adjacent sites. Inset: PDF for $U = 19.79$, with clearly observed tunneling oscillations.

*Tunneling oscillations:* For $n = 1$ the amplitude of Bloch oscillations is less than one site if $E \geq 10$ [7]. Thus, for $n \geq 2$ and increasing values of $U$, the amplitude of fractional Bloch oscillations will be less than one site if $EU^{n-1}(n-1)! \geq 10$. Then, $n$ particles launched on the same lattice site $p$ will be localized on that site for all times. The energy of that state will be $n((n-1)U/2 + pE)$. If however one particle will be moved to a different location with site $q$, then the energy would change to $(n-1)((n-2)U/2 + pE) + qE$. For specific values of $U$ these two energies will be equal:

$$(n-1)U = dE \ , \ d = q - p \ . \tag{15}$$

In such a case, one particle will leave the interacting cloud at site $p$ and tunnel to site $q$ at distance $d$ from the cloud, then tunnel back and so on, following effective Rabi oscillation scenario between the states $p, p\rangle$ and $|p, q\rangle$. This process will appear as an asymmetric oscillation of a fraction of the cloud either up or down the field gradient (depending on the sign of $U$). We calculate the tunneling splitting of these two states using higher order perturbation theory, for an example see Ref.[15]. The tunneling time is then obtained as

$$\tau_{tun} \simeq \frac{\pi}{\sqrt{n}} E^{d-1}(d-1)! \ . \tag{16}$$

In order to observe these tunneling oscillations, we compute the time averaged second moment $\overline{m_2} = \sum_j j^2 P_j(t) - \left(\sum_j j P_j(t)\right)^2$ of the PDF $P$. Then an effective time-averaged volume of the interacting cloud is taken to be $L = \sqrt{12\overline{m_2}} + 1$. We launch $n = 2$ particles at site $p = 40$ and plot the ratio $L(U)/L(U = 0)$ in Fig.4 (blue solid line). We find pronounced peaks at $U = E, 2E, 3E, 4E$ which become sharper and higher with increasing value of $U$. As a comparison we also compute the same ratio for the initial condition when both particles occupy neighbouring sites (dashed red line), for which the resonant structures are absent. According to the above, the resonant structures correspond to a tunneling of one of the particles to a site at distance $d = 1, 2, 3, 4$. The width of the peaks is inversely proportional to the tunneling time $\tau_{tun}$, and the height increases linearly with the tunneling distance $d$. In the inset in Fig.4, we plot the time evolution of the PDF $P_j$ for $U = 19.79$. We observe a clear tunneling process from site $p = 40$ to site $q = 44$. The numerically observed tunneling time is approximately 1730 time units, while our above prediction (16) yields $\tau_{tun} \approx 1666$, in very good agreement with the observations.

*Conclusions.* The above findings can be useful for control of the dynamics of interacting particles. They can be also used as a testbed of whether experimental studies deal with quantum many body states. One such testbed is the observation of fractional Bloch oscillations, another one is the resonant tunneling of a particle from an interacting cloud. An intriguing question is the way these quantum coherent phenomena will disappear in the limit of many particles, where classical nonlinear and nonintegrable wave mechanics are expected to take over.

*Acknowledgements.* R. Kh. acknowledges financial support of the Georgian National Science Foundation (GrantNo GNSF/STO7/4-197).

[1] F. Bloch, Z. Phys. **52**, 555 (1928); C. Zener, Proc. R. Soc. London, Ser. A **145**, 523 (1934); G.H. Wannier, Rev. Mod. Phys. **34**, 645 (1962).
[2] B.P. Anderson, M.A. Kasevich, Science **282**, 1686 (1998); M. Ben Dahan *et al*, Phys. Rev. Lett. **76**, 4508 (1996); O. Morsch *et al*, Phys. Rev. Lett. **87**, 140402 (2001); G. Ferrari *et al*, Phys. Rev. Lett. **97**, 060402 (2006).
[3] T. Pertsch *et al*, Phys. Rev. Lett. **83**, 4752 (1999); H. Trompeter *et al*, Phys. Rev. Lett. **96**, 023901 (2006); F. Dreisow *et al*, Phys. Rev. Lett. **102**, 076802 (2009).
[4] H. Sanchis-Alepuz *et al*,, Phys. Rev. Lett. **98**, 134301 (2007); L. Gutierrez *et al*, Phys. Rev. Lett. **97**, 114301 (2006);
[5] M. Gustavsson *et al*, Phys. Rev. Lett. **100**, 080404 (2008).
[6] P.K. Datta and A.M. Jayannavar, Phys. Rev. B 58, 8170 (1998).
[7] D.O. Krimer, R. Khomeriki, S. Flach, Phys. Rev. E, **80**, 036201 (2009).
[8] A. R. Kolovsky, E. A. Gomez EA and H. J. Korsch, Phys. Rev. A **81**, 025603 (2010)
[9] K. Winkler, *et al*, Nature, **441**, 853 (2006); W.C. Bakr, *et al*, Nature, **462**, 74 (2006);
[10] W. S. Dias, *et al*, Phys. Rev. B, **76**, 155124 (2007).
[11] A. Buchleitner, A.R. Kolovsky, Phys. Rev. Lett. **91**, 253002 (2003).
[12] M. Abramowitz, I.A. Stegun, *Handbook of Mathematical Functions* (1972).
[13] H. Fukuyama, R.A. Bari, H.C. Fogedby, Phys. Rev. B **8** 5579 (1973); P. Feuer, Phys. Rev., **88**, 92 (1952).

[14] A.C. Scott, J.C. Eilbeck, H. Gilhoj, Physica D, **78**, 194 (1994)

[15] S. Aubry et al, Phys. Rev. Lett. **76**, 1607 (1996).

# Impact of nonlinearity on Anderson and Wannier-Stark localization


**Dmitry Krimer[1], Sergej Flach[1], Haris Skokos[1], Ramaz Khomeriki[1,2] and Stavros Komineas[3]**

[1]Max-Planck-Institut für Physik komplexer Systeme, Nöthnitzer Str. 38, 01187 Dresden, Germany
[2]Physics Department, Tbilisi State University, Chavchavadze 3, 0128 Tbilisi, Georgia
[3]Department of Applied Mathematics, University of Crete, GR-71409, Heraklion, Crete, Greece



Linear wave equations with spatial disorder exhibit Anderson localization. Replacing the disorder by a dc field, Wannier-Stark localization occurs resulting in well-known Bloch oscillations. We study the fate of localized states in the presence of nonlinearity. In the case of disorder and for strong nonlinearity, there is a selftrapping of a part of the packet, and subdiffusion of the remainder [1-3]. In the case of dc bias, we found a long lived trapped regime with an explosive transition to Bloch oscillations, followed by a subdiffusive spreading at large time scales [4]. In all other cases wave localization is ultimately destroyed by nonlinearity. Our studies might be applicable to different systems such as Bose-Einstein condensates in optical lattices, the propagation of light waves in structured waveguide networks and photonic lattices.


## Wave packet evolution for Nonlinear Schrödinger and anharmonic oscillator chain with disorder

### Model I: DNLS chain

$$\mathcal{H}_D = \sum_l \epsilon_l |\psi_l|^2 + \frac{\beta}{2}|\psi_l|^4 - (\psi_{l+1}\psi_l^* + \psi_{l+1}^*\psi_l)$$

$$i\dot{\psi}_l = \epsilon_l \psi_l + \beta|\psi_l|^2\psi_l - \psi_{l+1} - \psi_{l-1}$$

$\epsilon_l$ : on-site energies distributed uniformly in $\left[-\frac{W}{2}, \frac{W}{2}\right]$

### Model II: Anharmonic oscillator chain

$$\mathcal{H}_K = \sum_l \frac{p_l^2}{2} + \frac{\tilde{\epsilon}_l}{2}u_l^2 + \frac{1}{4}u_l^4 + \frac{1}{2W}(u_{l+1}-u_l)^2$$

$$\ddot{u}_l = -\tilde{\epsilon}_l u_l - u_l^3 + \frac{1}{W}(u_{l+1}+u_{l-1}-2u_l)$$

$\tilde{\epsilon}_l$ : are chosen uniformly in $\left[\frac{1}{2}, \frac{3}{2}\right]$

### Wave packet characterization

$(\beta = 0)$ Ansatz: $\psi_l = A_l \exp(-i\lambda t)$

Eigenvalue problem : $\lambda A_l = \epsilon_l A_l - A_{l-1} - A_{l+1}$

Eigenvectors or normal modes (NMs): $A_{\nu,l}$

Eigenvectors are localized (Anderson localization [5])

Eigenfrequency spectrum: $\lambda_\nu \in \left[-2-\frac{W}{2}, 2+\frac{W}{2}\right]$

Width of the spectrum: $\Delta = W + 4$

Localization volume of NMs : $p_\nu = 1/\sum_l A_{\nu,l}^4$

Average spacing of eigenvalues of NMs within the range of localization volume : $\overline{\Delta\lambda} \approx \Delta/\overline{p_\nu}$

General solution in NM space: $\psi_l = \sum_\nu \phi_\nu A_{\nu,l}$

Normalized distribution: $z_\nu \equiv |\phi_\nu|^2/\sum_\mu |\phi_\mu|^2$

Participation number: $P = 1/\sum_\nu z_\nu^2$

Second moment: $m_2 = \sum_\nu (\nu-\bar{\nu})^2 z_\nu$ with $\bar{\nu} = \sum_\nu \nu z_\nu$

Compactness index: $\zeta = \frac{P^2}{m_2}$

SABA symplectic integrators are used for numerical simulations

### Regimes of spereading

Single site excitation: $\psi_l = \delta_{l,l_0}, \epsilon_{l_0} = 0$ Nonlinear frequency shift: $\delta_l = \beta|\psi_l|^2$

Three dynamical regimes: I) weak nonlinearity regime [1,6]; II) intermediate regime [1,6] and III) selftrapping regime [1,2] with I) $\delta_l < \overline{\Delta\lambda}$; II) $\overline{\Delta\lambda} < \delta_l < \Delta$; III) $\Delta < \delta_l$ [1]

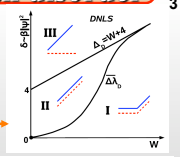


Schematic phase diagram. For each phase the dependence of log($m_2$) (blue solid curves) and of log P (red dashed curves) versus log t are shown.

$m_2$ and P vs. t in log-log plots with W=4 and β=0, 0.1, 1, 4.5 ((o)range,(b)lue, (g)reen, (r)ed). [Dashed lines: exponents 1/3 ($m_2$) and 1/6 (P)]. *Inset*: ς versus t for β=1.

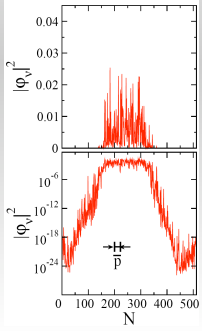


Norm density distributions at time t=$10^8$ for the regime II (W=4, β=1). The maximal mean value of the localization volume of the NMs <p>~22.

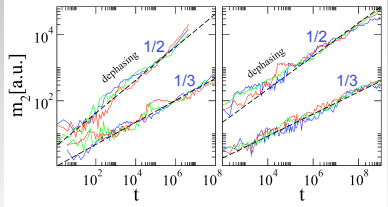


$m_2$ and P versus t in log-log plots for different values of W. Lower set of curves: no dephasing. Upper set of curves: with dephasing. Left panel: DNLS model. Right panel: Oscillator chain.

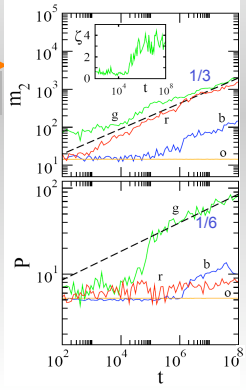


### Spreading mechanism

Cold exterior is incoherently heated by the packet; a part of the modes inside the packet evolve chaotic [1]

Equations of motion in NM space

$$i\dot{\chi}_\nu = \beta \sum_{\nu_1,\nu_2,\nu_3} I_{\nu,\nu_1,\nu_2,\nu_3}\chi_{\nu_1}^*\chi_{\nu_2}\chi_{\nu_3} e^{i(\lambda_\nu+\lambda_{\nu_1}-\lambda_{\nu_2}-\lambda_{\nu_3})t}$$

with the overlap integrals

$$I_{\nu,\nu_1,\nu_2,\nu_3} = \sum_l A_{\nu,l}A_{\nu_1,l}A_{\nu_2,l}A_{\nu_3,l}$$

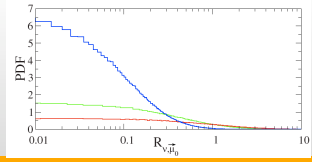


### Mode-mode resonances inside the packet

A NM with $|\phi_\nu|^2 = n$ is excited by a triplet of other modes

$\vec{\mu} \equiv (\mu_1, \mu_2, \mu_3)$ in first order in β as $|\phi_\nu^{(1)}| = \beta n^{3/2} R_{\nu,\vec{\mu}}^{-1}$ , $R_{\nu,\vec{\mu}} \sim \left|\frac{\vec{d\lambda}}{I_{\nu,\mu_1,\mu_2,\mu_3}}\right|$

with $\vec{d\lambda} = \lambda_\nu + \lambda_{\mu_1} - \lambda_{\mu_2} - \lambda_{\mu_3}$ , $R_{\nu,\vec{\mu}_0} = \min_{\vec{\mu}} R_{\nu,\vec{\mu}}$

Resonances set in if $\sqrt{n} < |\phi_\nu^{(1)}|$

The probability for a mode to be resonant with at least one other mode $\mathcal{P} = \int_0^{\beta n} \mathcal{W}(x)\mathrm{d}x \approx C\beta n$

Therefore $m_2 \sim C^{2/3}\beta^{4/3}t^\alpha$ , $\alpha = 1/3$

Statistical properties of NMs.
Probability densities $\mathcal{W}(R_{\nu,\vec{\mu}_0})$ of NMs being resonant.
Disorder strength W=4,7,10 (from top to bottom)

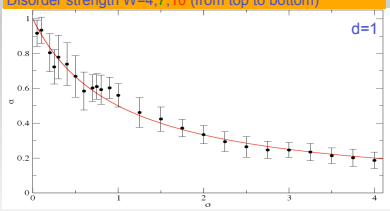


Exponent α ( $m_2 \sim t^\alpha$ ) versus order of nonlinearity σ for $u_l^3 \to |u_l|^\sigma u_l$ [3]. Red curve: theoretical prediction $\alpha = 1/(1+d\sigma)$ [1].

## Wave packet evolution for Nonlinear Schrödinger chain with dc bias (Stark ladder)

$$\mathcal{H}_D = \sum_l lE|\psi_l|^2 + \frac{\beta}{2}|\psi_l|^4 - (\psi_{l+1}\psi_l^* + \psi_{l+1}^*\psi_l)$$

$E$ : strength of dc field

Equation: $i\dot{\psi}_l = -(\psi_{l+1}+\psi_{l-1}) + lE\psi_l + \beta|\psi_l|^2\psi_l$

Eigenvalue problem (β=0): $\lambda A_l = lEA_l - A_{l-1} - A_{l+1}$

Normal modes (NM) $A_{\nu,l}$ are localized (Wannier-Stark states [7]) Translational invariance: $A_{l+\mu}^{(\nu+\mu)} = A_l^{(\nu)}$

$A_l^{(0)} = J_l(2/E)$, $J_l(x)$: Bessel function of the first kind

Eigenvalues form equidistant spectrum: $\lambda_\nu = E\nu$

Localization volume of NM $\mathcal{L} = 1/\sum_l |A_l^{(0)}|^4$

Frequency scales: Eigenvalue spacing: $E$

The eigenvalue variation over a localization volume: $\Delta \equiv E\mathcal{L}$

Period of Bloch oscillations: $T_B = 2\pi/E$

### Regimes of spreading

Single site excitation: $\psi_l = \delta_{l,l_0}$

Frequency shift of a single site oscillator: $\delta \equiv \beta$

Three different regimes of spreading [4]: (I) $\delta < E$; (II) $E < \delta < \Delta$; (III) $\Delta < \delta$

I: weak nonlinear regime (no initial resonance overlap with NMs)

II: intermediate regime (resonance overlap happens from the beginning)

III: trapped regime (δ tunes the excited site out of resonance with neighboring NMs)

Dashed line: Estimate of the transition to the trapped regime III using the dimer model

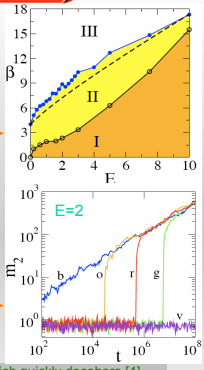


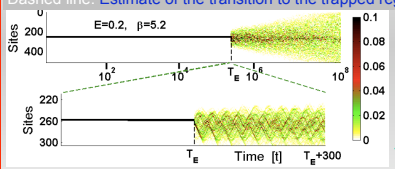


**Regime III: large nonlinearities.**

Excitation is trapped up to some time $T_E$ followed by explosive spreading. β=8,8.15 8.25 8.5 8.9 (b);(o) (g) (r); (v)

$10^8$ corresponds to $3.2\cdot10^7$ periods of $T_B$




For t>$T_E$ an explosive and spatially asymmetric spreading on a time scale of $T_B$. Then for about ~10 $T_B$ Bloch oscillations which quickly decohere [4]. Finally, subdiffusive behavior. Frequency shift δ>0 =>more effective interaction with the right site (asymmetry).


**References:**

[1] S. Flach, D.O. Krimer, Ch. Skokos, Phys. Rev. Lett. 102, 024101 (2009); Ch. Skokos, D.O. Krimer, S. Flach, S. Komineas, Phys. Rev. E 79, 056211 (2009)
[2] G. Kopidakis, S. Komineas, S. Flach, S. Aubry, Phys. Rev. Lett. 100, 084103 (2008)
[3] Ch. Skokos and S. Flach, in preparation
[4] D.O. Krimer, R. Khomeriki, S. Flach, (to appear in Phys. Rev. E) (2009)
[5] P. W. Anderson, Phys. Rev. 109, 1492 (1958)
[6] A. S. Pikovsky, D. L. Shepelyansky, Phys. Rev. Lett. 100, 094101 (2008)
[7] G. H. Wannier, Phys. Rev. 117, 432 (1960)

# Anderson Localization and Nonlinearity in Disordered and Incommensurate Photonic Lattices

**Y. Lahini[1], R. Pugatch[1], R. Morandotti[2], D. N. Christodoulides[3]**
**N. Davidson[1] and Y. Silberberg[1]**
[1]The Weizmann Institute of Science, Rehovot, Israel
[2]Institut National de la Recherche Scientifique, Varennes, Quebec, Canada
[3]CREOL/College of Optics, University of Central Florida, Orlando, Florida, USA

We present an experimental study of the transverse localization of light[1,2] in nonlinear a-periodic lattices. We describe the observation of exponential (Anderson) localization of expanding wavepackets and localized eigenmodes in disordered lattices, and an experimental study of the effect of weak nonlinearity on Anderson localization in one dimension[3]. The effect of nonlinearity is found to be highly dependent of the exact initial condition. We also present results for intensity correlation measurements that reveal underlying linear and nonlinear effects.

In a different set of experiments[4] we report the observation of the signature of a localization transition for light in one dimensional quasi-periodic photonic lattices[5], by directly measuring the expansion rates of initially narrow wave packets propagating in the lattice. Below the transition all the modes of the system are extended and therefore an initially narrow wave-packet eventually spreads across the entire lattice. Above the critical point, all modes are localized and expansion is suppressed. In addition, we measure the effect of focusing nonlinear interaction on the propagation and find it increases the width of the localized wave-packets.

**REFERENCES**

1. H. De Raedt et. al., Phys. Rev. Lett. **62**, 47 (1989)
2. T. Schwartz et. al., Nature **446**, 53 (2007)
3. Y. Lahini et al., Phys. Rev. Lett. **100**, 013906 (2008)
4. Y. Lahini, R. Pugatch et al., Phys. Rev. Lett. **103**, 013901 (2009)
5. S. Aubry and G. Andre, Ann. Israel. Phys. Soc. 3, **133** (1980).

# Evolution of wave packets in nonlinear disordered media: strong chaos and asymptotic weak chaos spreading regimes

T.V. Laptyeva, J.D. Bodyfelt, D.O. Krimer, Ch. Skokos, and S. Flach

*Max Planck Institute for the Physics of Complex Systems, Nothnitzer Str. 38, 01187 Dresden, Germany*

Recent studies suggest that the wave packet spreading in 1D disordered systems with cubic nonlinearities is characterized by an asymptotic divergence of the second moment $m_2$ in time, as $t^{1/3}$ [1,2]. We find a qualitatively new dynamical intermediate regime, where the second moment spreads faster (as $t^{1/2}$), with a crossover to the asymptotic $m_2 \sim t^{1/3}$ law at larger times [3]. The phenomenon is attributed to the strong chaos regime, in contrast to the previously observed weak chaos. The crossover between the regimes is controlled by the ratio of nonlinear frequency shifts and the average eigenvalue spacing of eigenstates of the linear equations within one localization volume. We analyze the details of the different spreading regimes performing extensive numerical simulations with variations of the disorder strength and initial wave packet amplitude.

[1] S. Flach, D.O. Krimer, Ch. Skokos, *Phys. Rev. Lett.* **102,** 024101 (2009).
[2] Ch. Skokos, D.O. Krimer, S. Komineas, S. Flach, *Phys. Rev. E* **79**, 056211 (2009).
[3] S. Flach, *Chem. Phys.,* in print, arXiv 1001.2673v1 (2010).

**Keywords:** disorder, Anderson localization, nonlinearity, chaos, diffusion
**PACS:** 05.45-a, 05.60Cd, 63.20Pw

# Experimental observation of the Anderson transition with matter waves

**Team:** *Systèmes quantiques complexes*
Gabriel Lemarié, Benoît Grémaud and Dominique Delande

Laboratoire Kastler Brossel — Physique quantique et applications

**Collaboration:** Julien Chabé, Pascal Szriftgiser and Jean Claude Garreau (Laboratoire PHLAM, Lille)

Comité AERES 2009

## Unusual transport properties predicted for disordered materials

### Anderson localization

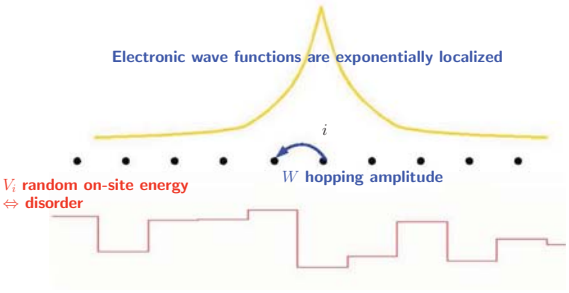


Interplay between disorder and interference effects

### The Anderson Metal-Insulator transition [6]

- In 3D, a disorder-induced phase transition is predicted (ome parameter scaling theory).
- Few experimental results (decoherence sources, interactions, optical absorptions).

## Quantum simulation of the 3D-Anderson model using the quasi-periodic Kicked Rotor

### The Kicked Rotor with cold atoms [2]

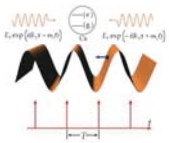

$$\hat{H} = \frac{\hat{p}^2}{2} + k\cos\hat{\theta}\,\Sigma_n\,\delta(t-nT)$$

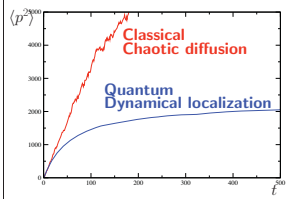


Fig. 1: **Dynamical localization**: $K = kT = 10$, $\hbar_{\text{eff}} = 2.89$. $E_k \sim < p^2 >$ is averaged over 400 initial conditions.

- $K = kT$ large ⇒ **classical dynamics is chaotic**: $\langle p^2\rangle \sim Dt$
- At long times, the quantum dynamics freezes: **localization in momentum space**
- **Kicked Rotor dynamics ≡ 1D-Anderson model** [3]: momentum $p \equiv$ site $i$

### The quasiperiodic Kicked Rotor

$$\hat{H} = \frac{\hat{p}^2}{2} + k\cos\hat{\theta}\,[1+\epsilon\cos(\omega_1 t)\cos(\omega_2 t)]\,\Sigma_n\,\delta(\omega_0 t - n)$$

- $\omega_0$, $\omega_1$ and $\omega_2$, incommensurate frequencies ⇒ new dimensions in the extended phase-space.
- **Quasiperiodic Kicked Rotor dynamics ≡ 3D Anderson model** [5].

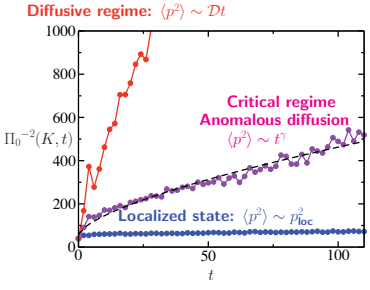


Fig. 2: **Experimental** observation of the crossover from a localized state to a diffusive regime. Close to the critical point, it displays at long time a power law characteristic of an anomalous diffusion. This singular behavior is a signature of the vicinity of the Anderson transition.

- Experimentally, it is much easier to measure the population $\pi_0(t)$ of the zero velocity class
- By virtue of the constancy of the total number of atoms
  - $\Pi_0(K,t) \propto p_{\text{loc}}^{-1}$ in the localized regime
  - $\Pi_0(K,t) \propto \langle p^2\rangle^{-1/2}$ in the localized regime

## Experimental observation of the Anderson transition

PRL 101, 255702 (2008); Physics 1, 41 (2008).

### Phase-diagram of the quasi-periodically kicked rotor

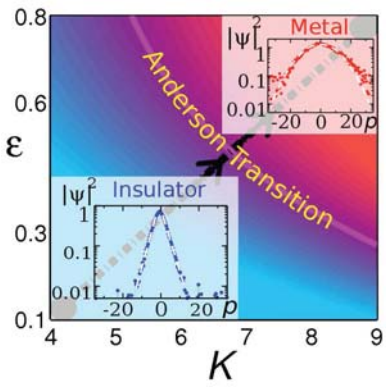


Fig. 3: The insets show the **experimentally observed** momentum distributions. In the localized regime (blue curve), the distribution is exponentially localized resulting in approximately straight lines in the semilog plot. In the diffusive regime (red curve), the distribution is Gaussian (parabola in the semilog plot). The experimental parameters are swept along the black-dotted line going from $(K = 4, \epsilon = 0.1)$ to $(K = 9, \epsilon = 0.8)$.

### One parameter scaling hypothesis [7]

$$\Lambda = \frac{1}{\Pi_0^2(K,t)t^{2/3}} = F\left[\frac{\xi(K)}{t^{1/3}}\right]$$

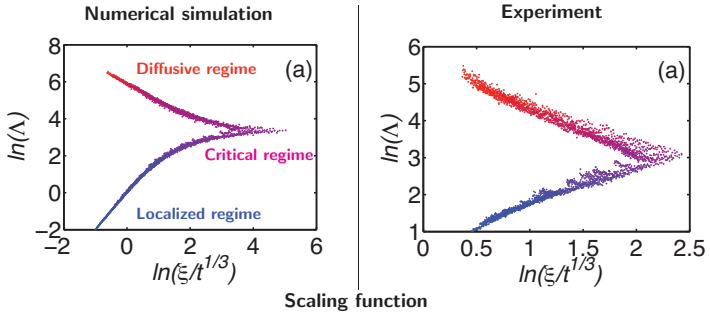


## First experimental measurement of the critical exponent of the Anderson transition

$$\frac{1}{\xi} = \alpha(K - K_c)^{\nu} + \beta(\eta)$$

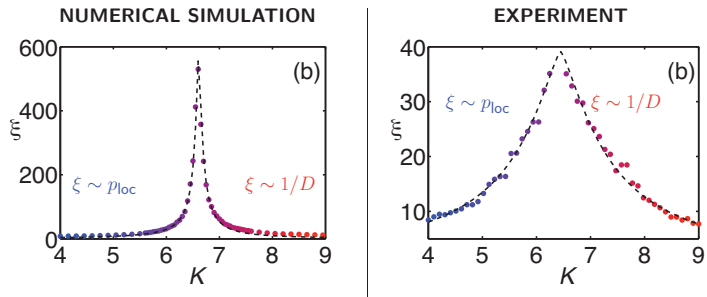


$\nu = 1.6 \pm 0.05,\ K_c \simeq 6.6$ | $\nu = 1.4 \pm 0.3,\ K_c \simeq 6.4$

**References**

[1] P.W. Anderson, *Physical Review* **109**, 1492 (1958).
[2] G. Casati and al., *Lect. Notes Phys.* **93**, 334 (1979).
[3] D. R. Grempel and al., *Phys. Rev. A* **29**, 1639 (1984).
[4] F. L. Moore and al., *Phys. Rev. Lett.* **75**, 4598 (1995).
[5] G. Casati and al., *Phys. Rev. Lett.* **63**, 345 (1989).
[6] B. Kramer and al., *Rep. Prog. Phys.* **56**, 1469 (1993).
[7] D. Stauffer and al., *Introduction to Percolation Theory*, (London 1994: Taylor and Francis).
[8] K. Slevin and al., *Phys. Rev. Lett.* **82**, 382 (1999).

**Cascade Picture and Extended Self-Similarity in Electron Localization**

Luca Moriconi

Instituto de Física, Universidade Federal do Rio de Janeiro,
C.P. 68528, Rio de Janeiro, RJ – 21945-970, Brasil

Abstract:

We show that extended self-similarity, a scaling phenomenon firstly observed in classical turbulent flows, holds for the two-dimensional metal-insulator transition in the universality classes of random Dirac fermions and the integer quantum Hall effect. Deviations from multifractality, which in turbulence are due to the dominance of diffusive processes at small scales, appear in the condensed matter context as a large scale, finite size effect related to the imposition of an infra-red cutoff in the field theory formulation. We propose a phenomenological interpretation of extended self-similarity in the metal-insulator transition within the framework of the random β-model description of multifractal sets.

In the specific case of the Quantum Hall metal-insulator transition, extended self-similarity is clearly verified despite the narrow spatial range where probability structure functions exhibit multifractal scaling for small lattices. As finite size effects get stronger for structure functions with negative orders, the parabolic approximation for the multifractal spectrum loses accuracy. However, taking profit of extended self-similarity, an improved evaluation of the multifractal exponents is attained for negative orders too, rendering them consistent with previous results, which rely on computations performed for considerably larger systems.

# Localization in Systems with Disorder and Strong Nonlinearity

Mario Mulansky and Arkady Pikovsky
Institute of Physics and Astronomy, University of Potsdam

## The Model

Discrete Anderson Nonliner Schrödinger Equation (DANSE) in one dimension

$$i\dot{\psi}_n = \psi_{n+1} + \psi_{n-1} + V_n\psi_n + |\psi_n|^{2\alpha}\psi_n$$

- $\alpha = 0.5, 1, 2, 3$ : Nonlinearity Index
- $\alpha = 1$: usual DANSE model
- $-W/2 \leq V_n \leq W/2$ Random Potential (iid. random numbers)

Experimental realization e.g. in BECs [4], disordered photonic lattices [7] or coupled optical waveguides [3].

## Anderson Localization

Based on the results from Anderson [1]: In a linear, disordered lattice, every eigenfunction is exponentially localized. The plot shows a typical, localized eigenmode.

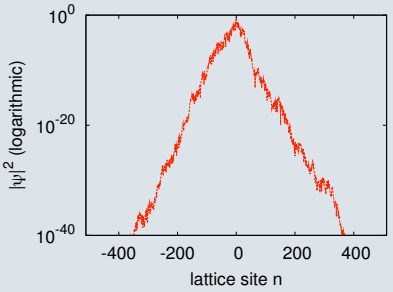


## Effects of Nonlinearity

For $\alpha = 1$, previous simulations showed subdiffusive spreading $(\Delta n)^2 \sim t^{0.35}$ [5]

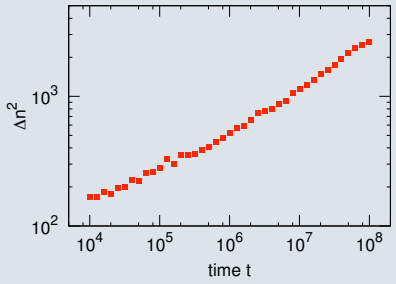


**Other $\alpha$: no results until now**

## Spreading Mechanism

- Spreading due to nonlinear mode interaction ⟶ nonlinear diffusion eq.:

$$\frac{\partial \rho}{\partial t} = \frac{\partial}{\partial x}\left(\rho^a \frac{\partial \rho}{\partial x}\right)$$

- solution $\rho \sim t^{-1/(2+a)} f(x/t^{1/(2+a)})$ leads to spreading:

$$(\Delta n)^2 \sim t^\gamma \quad \text{with} \quad \gamma = 2/(a+2)$$

- Relation between $a$ and $\alpha$ unclear
- *"strong stochasticity"*
  $a = 2\alpha \rightarrow \gamma_A = 1/(1+\alpha)$
- *"weak stochasticity"*
  $a = 3\alpha \rightarrow \gamma_B = 2/(2+3\alpha)$
- *"very weak stochasticity"*
  $a = 4\alpha \rightarrow \gamma_C = 1/(1+2\alpha)$

## Numerical Results

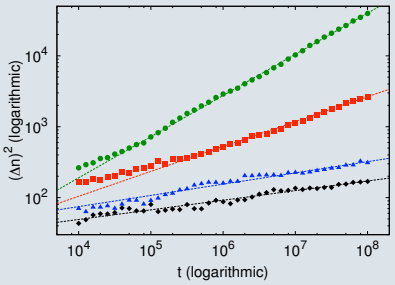


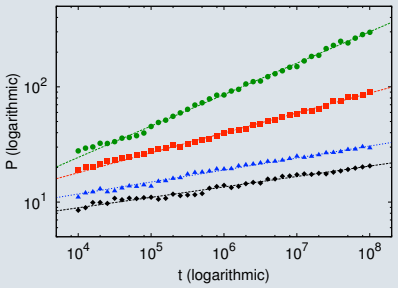


| $\alpha$ | 0.5 (green) | 1 (red) | 2 (blue) | 3 (black) |
|---|---|---|---|---|
| $\gamma$ from fit $(\Delta n)^2 \sim t^\gamma$ | $0.56 \pm 0.04$ | $0.31 \pm 0.04$ | $0.18 \pm 0.04$ | $0.14 \pm 0.05$ |
| $\gamma$ from fit $P \sim t^{\gamma/2}$ | $0.53 \pm 0.05$ | $0.33 \pm 0.05$ | $0.21 \pm 0.06$ | $0.18 \pm 0.06$ |
| $\gamma_A$ (strong stochasticity) | 0.67 | 0.50 | 0.33 | 0.25 |
| $\gamma_B$ (weak stochasticity) | 0.56 | 0.40 | 0.25 | 0.18 |
| $\gamma_C$ (very weak stochasticity) | 0.50 | 0.33 | 0.20 | 0.14 |

## Structural Entropy

Participation Number $P$:

$$P^{-1} := \sum_n |\psi_n|^4$$

Rényi entropies:

$$I_q := \frac{1}{1-q} \ln \sum_n |\psi_n|^{2q}$$

- $I_1 = S$ deviation from uniform distrib.
- $I_2 = \ln P$ spatial extend
- $S = \ln P + S_{str}$: assumes that deviation from unif. distr. is due to limited spatial extend and complex peak structure [6], hence

$$S_{str} := S - \ln P$$

## Spreading States

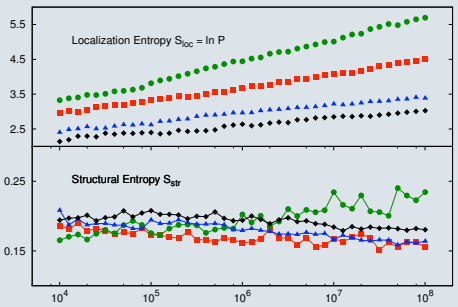


Peak structure remains nearly constant while the wavefunction spreads

## Summary and Conlusion

- The numerical results for the generalized DANSE model seem to support very weak and/or weak stochasticity assumptions which was also found by Flach et al. [2].
- Reasons for this downscale are still unclear – studies on finite time Lyapunov exponents might give more insights.
- Structural Entropy shows that the peak structure of spreading wavefunctions does not change.
- Consequently, one could also use normal entropy $S$ as a measure of localization.

## References

[1] P. W. Anderson, *Absence of diffusion in certain random lattices*, Physical Review Letters **109** (1958), no. 5, 1492–1505.

[2] S. Flach, D. O. Krimer, and Ch. Skokos, *Universal spreading of wave packets in disordered nonlinear systems*, Physical Review Letters **102** (2009), no. 2, 024101.

[3] D. Hennig and G. P. Tsironis, *Wave transmission in nonlinear lattices*, Physics Reports **307** (1999), no. 5-6, 333–432.

[4] J. E. Lye, L. Fallani, M. Modugno, D. S. Wiersma, C. Fort, and M. Inguscio, *Bose-Einstein condensate in a random potential*, Physical Review Letters **95** (2005), no. 7, 070401.

[5] A. S. Pikovsky and D. L. Shepelyansky, *Destruction of Anderson localization by a weak nonlinearity*, Physical Review Letters **100** (2008), no. 9, 094101.

[6] János Pipek and Imre Varga, *Universal classification scheme for the spatial-localization properties of one-particle states in finite, d-dimensional systems*, Physical Review A **46** (1992), no. 6, 3148–3163.

[7] Diederik S. Wiersma, Paolo Bartolini, Ad Lagendijk, and Roberto Righini, *Localization of light in a disordered medium*, Nature (1997), 671–673.

http://www.stat.physik.uni-potsdam.de mulansky@uni-potsdam.de

# Thermalization in short Random Nonlinear Lattices

Karsten Ahnert[1], Mario Mulansky[1], Arkady Pikovsky[1] and Dima Shepelyansky[2]

[1]University of Potsdam, [2]Université de Toulouse

## Introduction

We study the Discrete Anderson Nonlinear Schrödinger Equation (DANSE)

$$i\dot{\Psi}_n = \Psi_{n+1} + \Psi_{n-1} + V_n\Psi_n + \beta|\Psi_n|^2\Psi_n$$

In the linear system ($\beta = 0$), all eigenmodes are exponentially localized with localization length $\xi \approx 96W^{-2}$.

With $\beta > 0$, the interplay between disorder and nonlinearity can be studied.

Experimental realizations in:

- wave guide arrays, or
- Bose Einstein condensates.

We investigate the thermalization properties: The evolution of initially localized states to a thermal equilibrium.

## The Model

The DANSE possesses the following properties:

- Disorder: $-W/2 \leq V_n \leq -W/2$ iid. random numbers
- Nonlinearity: $\beta$
- Norm conservation $1 = \sum_n |\Psi_n|^2$
- Energy conservation $E(t) = E(0)$

Numerical integration of the lattice equations is performed using a Crank-Nicolson operator splitting scheme with $\Delta t = 0.1$. Periodic boundary conditions have been used and the lattice is in relatively short, $N = 16, 32, 64$.

## Eigenmode representation

We use the eigenmode representation

$$\Psi_n = \sum_m C_m \phi_{mn}$$

where $\phi_{mn}$ is the $m$-th eigenmode of the disordered linear lattice. In this representation the model reads

$$i\dot{C}_m = \epsilon_m C_m + \beta \sum_{i,j,k} V_{m,i,j,k} C_i^\star C_j C_k \,,$$

with eigenenergies $\epsilon_m$ and overlap $V_{m,i,j,k}$.

**Initial conditions:** $C_m(t=0) = \delta_{m,m'}$

## Entropy

The standard entropy

$$S = -\sum_m p_m \ln p_m \quad \text{with} \quad p_m = \langle |C_m|^2 \rangle_t$$

measures localization. $\langle\cdot\rangle_t$ means time averages over small time windows.

Time evolution of the entropy ($N = 32$):

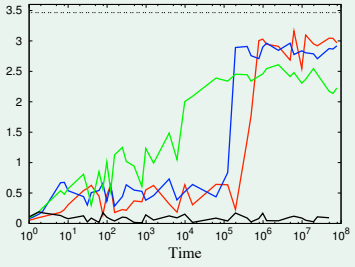


green: E=1.79, blue: E=1.13, red: E=0.57, black: E=3.13

## Thermalization

Because of the energy and norm conservation, thermalization is not given by complete equipartition between the modes ($S = \ln N$). An estimation of $p_m$ can be obtained from the linear lattice. From the maximization of $S$ follows the Gibbs distribution

$$p_m = \frac{1}{Z}\exp\left(-\epsilon_m/T\right).$$

and the entropy $\langle S_{Gibbs}\rangle = \langle E\rangle/T + \langle \ln Z\rangle$.

Averaging over disorder realizations gives

$$\langle \ln Z\rangle \approx \ln N + \ln\sinh(\Delta/T) - \ln(\Delta/T)$$

and $\langle E\rangle = T^2\partial\langle \ln Z\rangle/\partial T$, where $\Delta$ are the borders of the spectrum: $\Delta \approx 3.0$ for $W = 4.0$.

Entropy in dependence of state energy (normalized according to $\sum_m \epsilon_m = 0$). States with entropies close to the theoretical value $\langle S_{Gibbs}\rangle$ are considered as thermalized.

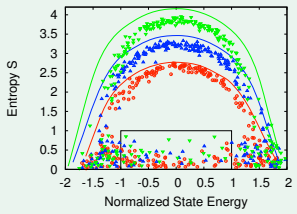


green: N=64, blue: N=32, red: N=16, Solid lines: $\langle S_{Gibbs}\rangle$

**Some of the initially excited modes do not thermalize.**

## (Non)Thermalization and Bifurcation

Fraction $f_{th}$ of the initial states which are thermalized after $t = 10^6$ for different values of the nonlinearity $\beta$ (top panel).

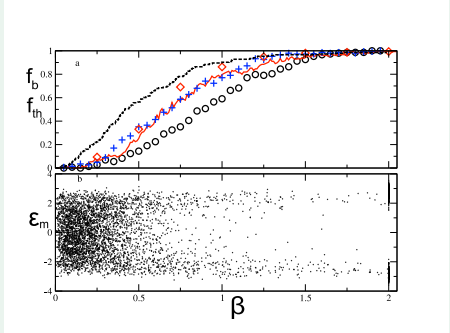


$N = 16$ (black circles), 32 (red line), 64 (blue pluses). Red diamonds are $N = 32, t = 10^7$. Dashed black are bifurcated breathers $f_b$ (see text on the right).

**Why do some initially excited eigenmodes thermalize and others don't?**

Possible explanation via bifurcation of breathers: Solutions of the linear problem (eigenmodes) might be continued for increasing nonlinearity $\beta > 0$.

Numerical method: Look for solutions of the DANSE of the form $\psi_n(t) = \phi_n e^{-i\epsilon t}$. This leads to a nonlinear eigenvalue problem: $\epsilon\phi_n = E_n\phi_n + \beta\phi_n^3 + \phi_{n-1} + \phi_{n+1}$ that has a solution at $\beta = 0$: the eigenmode. Starting from this eigenmode, the solution can be continued until some $\beta_C$ where it bifurcates and becomes unstable. This gives a number of bifurcated states $f_b(\beta)$ that can be compared to the number of thermalized states $f_{th}$ (top graph on the left).

## Summary

We have studied the thermalization properties of the DANSE.

- Emergence of dynamical localization with Gibbs distribution above a certain border for nonlinearity strength was established.
- Some states do not thermalize during the time evolution. As time increases, the number of thermalized states increases.
- Nonthermalized states can be explained by stable breathers emerging from the linear eigenmodes.
- If the eigenmode bifurcates at some value of $\beta = \beta_C$, one can expect thermalization of this mode for $\beta > \beta_C$.

# Suppression of Anderson localization of light and Brewster anomalies in disordered superlattices containing a dispersive metamaterial

**F. A. Pinheiro[1,*], D. Mogilevtsev[2,3], R. R. dos Santos[1], S. B. Cavalcanti[4], and L. E. Oliveira[2]**

*[1] Instituto de Física, Universidade Federal do Rio de Janeiro, Caixa Postal 68528, 21941-972, Brazil*

*[2] Instituto de Física, UNICAMP, CP 6165, Campinas-SP, 13083-970, Brazil*

*[3]Institute of Physics, NASB, F. Skarina Ave. 68, Minsk, 220072, Belarus*

*[4]Instituto de Física, Universidade Federal de Alagoas, Maceió-AL, 57072-970, Brazil*

***E-mail: fpinheiro@if.ufrj.br***

Light propagation through 1D disordered structures composed of alternate layers, with random thicknesses, of air and a dispersive metamaterial is theoretically investigated. Both normal and oblique incidences are considered. By means of numerical simulations and an analytical theory, we have established that Anderson localization of light may be suppressed: (i) in the long wavelength limit, for a finite angle of incidence which depends on the parameters of the dispersive metamaterial; (ii) for isolated finite frequencies, and for specific angles of incidence, corresponding to Brewster anomalies in both positive- and negative-refraction regimes of the dispersive metamaterial. These results suggest that Anderson localization of light could be explored to control and tune light propagation in disordered metamaterials.

# Statistics of Wavefunctions at Anderson Transition in Power-Law Random Banded Matrices

ILIA RUSHKIN

Power-law random banded matrices describe a tight-banding model with long-ranged random hopping. Depending on the decay rate of the hopping probability with the distance, the system undergoes the Anderson transition, even in 1D. The wavefunctions at the transition are believed to have multifractal statistics. This is verified in the first two orders of perturbation series in the wide band limit, and the subleading correction to the multifractal spectrum is found. The result suggests that the expected duality relation $d_b+d_{1/b}=1$ between the multifractal dimensions in the wide and narrow band limits is not exact. A similar calculation is done for the ensemble of ultrametric random matrices.

**Lev RYASHKO**

# STABILITY AND CONTROL FOR INVARIANT MANIFOLDS OF NONLINEAR STOCHASTIC SYSTEMS

Abstract

A mean square stability for the invariant manifolds of nonlinear stochastic systems is considered. The first approximation linear systems for invariant manifolds are introduced and a notion of P-stability (projective) is proposed. A criterion for P-stability is obtained. Mean square stabilization of periodic and quasiperiodic solutions of stochastically forced nonlinear systems is considered. The necessary and sufficient stabilizability conditions are presented. The methods for design of feedback stabilizing regulator for SDEs are suggested. The examples of constructive solving of stochastic control problem are demonstrated. An application of this theory to the analysis of turbulence is discussed.

Band center anomaly and single parameter scaling in one-dimensional Anderson localization

# Decay of turbulence in rotating flows

T. Teitelbaum[1], P.D. Mininni [1,2], J. Baerenzung [3], D. Rosenberg [2], and A. Pouquet [2]
[1] *Departamento de Física, Facultad de Ciencias Exactas y Naturales, Universidad de Buenos Aires, IFIBA and CONICET, Ciudad Universitaria, 1428 Buenos Aires, Argentina.*
[2] *NCAR, P.O. Box 3000, Boulder, Colorado 80307-3000, U.S.A.*
[3] *Laboratoire des Écoulements Geophysiques et Industriels, CNRS and Université Joseph Fournier, BP53,F-38041, Grenoble cedex 9, France.*
(Dated: June 30, 2010)

We present a parametric space study of the decay of turbulence in rotating flows combining direct numerical simulations, large eddy simulations, and phenomenological theory. Several cases are considered: (1) the effect of varying the characteristic scale of the initial conditions when compared with the size of the box, to study "bounded" and "unbounded" flows; (2) the effect of helicity (correlation between the velocity and vorticity); (3) the effect of Rossby and Reynolds numbers; and (4) the effect of anisotropies in the initial conditions. Initial conditions include the Taylor-Green vortex, the Arn'old-Beltrami-Childress flow, and random flows with large-scale energy spectrum proportional to $k^4$. The decay laws obtained in the simulations for the energy, helicity, and enstrophy in each case can be explained with phenomenological arguments that separate the decay of two-dimensional from three-dimensional modes, and that take into account the role of helicity in slowing down the energy decay. The time evolution of the energy spectrum and development of anisotropies in the simulations is also discussed. Finally, the effect of rotation and helicity in the skewness and kurtosis of the flow is considered.

# Cascade Random Distributed Feedback Fiber Laser

Ilya D. Vatnik
*Institute of Automation and Electrometry, Novosibirsk, Russia*
*E-mail: vatnik_i@mail.ru*

## Rayleigh feedback in optic fiber

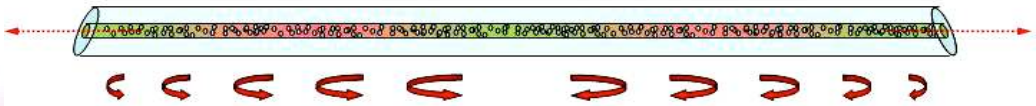

- Part of propagating radiation (0.01 % per kilometer) is scattered backward due to Rayleigh scattering by inhomogeneities within the glass structure.
- Backscattered light can be amplified somehow and sufficient feedback can be provided.

Generation in fiber for the anomalous dispersion regime caused by random distributed feedback has been demonstrated recently [S. K. Turitsyn et al., Random distributed feedback fibre laser, Nature Photonic 4, 231 - 235 (2010)].

*May lasing occur in the normal dispersion regime?*

## Experimental Setup

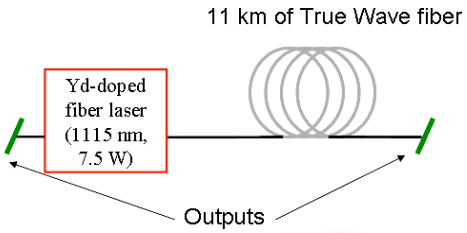


- Stimulated Raman scattering provides distributed amplification of backscattered radiation and results in lasing of first (~ 1173 nm) and also second (~ 1240 nm) Stocks component

## Results

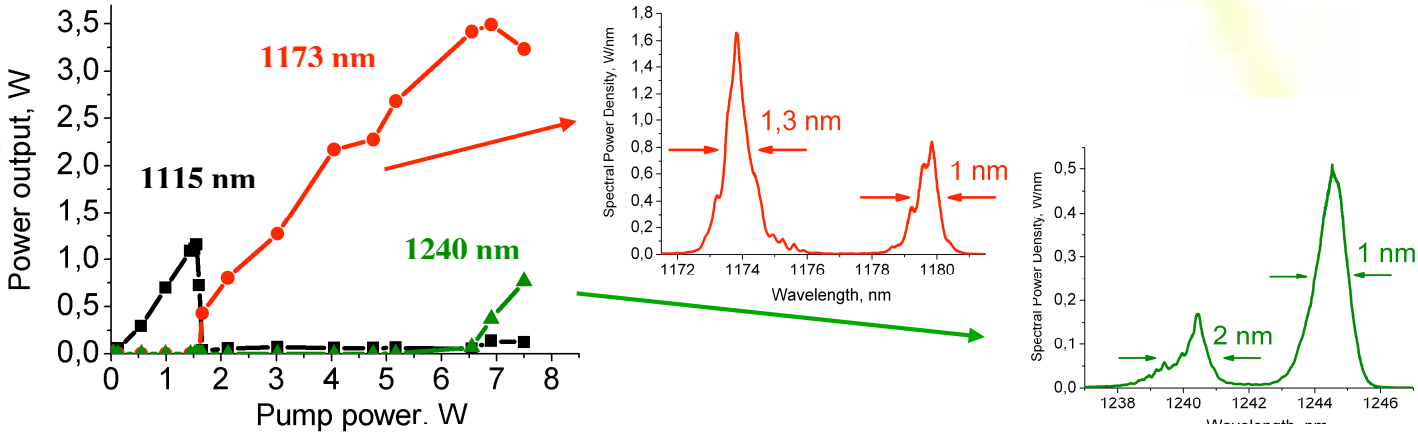


- ✓ High efficiency - up to 50%
- ✓ High power of the first Stocks component excites cascade lasing
- ✓ High-quality output beam – $M^2$~1.1

CW cascade generation in optic fiber led by random distributed rayleigh feedback has been demonstrated for the normal dispersion regime